Chem Soc Rev

REVIEW ARTICLE

View Article Online
View Journal | View Issue

Cite this: *Chem. Soc. Rev.*, 2015, **44**, 6616

Received 28th February 2015

DOI: 10.1039/c5cs00183h

www.rsc.org/chemsocrev

New advances in nanographene chemistry

Akimitsu Narita,[a] Xiao-Ye Wang,[a] Xinliang Feng[b] and Klaus Müllen*[a]

Nanographenes, or extended polycyclic aromatic hydrocarbons, have been attracting renewed and more widespread attention since the first experimental demonstration of graphene in 2004. However, the atomically precise fabrication of nanographenes has thus far been achieved only through synthetic organic chemistry. The precise synthesis of quasi-zero-dimensional nanographenes, *i.e.* graphene molecules, has witnessed rapid developments over the past few years, and these developments can be summarized in four categories: (1) non-conventional methods, (2) structures incorporating seven- or eight-membered rings, (3) selective heteroatom doping, and (4) direct edge functionalization. On the other hand, one-dimensional extension of the graphene molecules leads to the formation of graphene nanoribbons (GNRs) with high aspect ratios. The synthesis of structurally well-defined GNRs has been achieved by extending nanographene synthesis to longitudinally extended polymeric systems. Access to GNRs thus becomes possible through the solution-mediated or surface-assisted cyclodehydrogenation, or "graphitization," of tailor-made polyphenylene precursors. In this review, we describe recent progress in the "bottom-up" chemical syntheses of structurally well-defined nanographenes, namely graphene molecules and GNRs.

I. Introduction

After the first experimental demonstration of graphene, a monolayer of graphite, by Geim and Novoselov in 2004, numerous research groups with different backgrounds have investigated this material.[1–4] Graphene has been shown to have a variety of exceptional properties, particularly extremely high charge-carrier

[a] *Max Planck Institute for Polymer Research, Ackermannweg 10, 55128 Mainz, Germany. E-mail: muellen@mpip-mainz.mpg.de*
[b] *Center for Advancing Electronics Dresden (CFAED) & Department of Chemistry and Food Chemistry, Dresden University of Technology, Walther-Hempel-Bau Mommsenstrasse 4, 01062 Dresden, Germany*

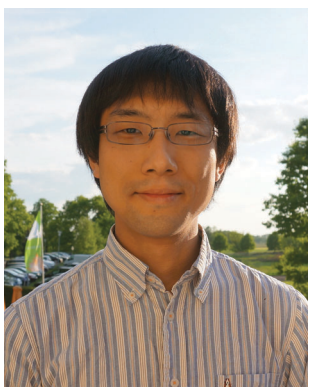

Akimitsu Narita

Akimitsu Narita was born in Yokohama, Japan in 1986. He received his Bachelor's (2008) and Master's (2010) degrees in Chemistry at the University of Tokyo under the supervision of Professor Eiichi Nakamura. In March 2014, he obtained his PhD in the group of Professor Klaus Müllen at the Max Planck Institute for Polymer Research (MPIP) in Mainz. He was an Early-Stage Researcher in the Marie-Curie Initial Training Network (ITN) "SUPERIOR" for three years from May 2010. Beginning in August 2014, he became a project leader in the Synthetic Chemistry Department at MPIP. His current research focuses on the bottom-up organic synthesis of functional graphene molecules and graphene nanoribbons.

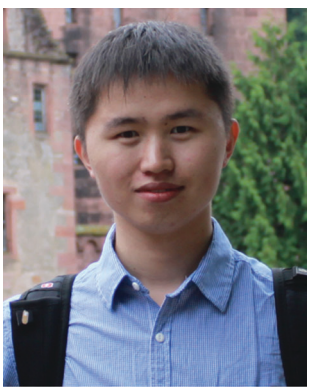

Xiao-Ye Wang

Xiao-Ye Wang was born in China in 1989. He received his Bachelor's degree in chemistry from Nankai University in 2009. In the same year, he joined Professor Jian Pei's group at Peking University as a graduate student and obtained his PhD degree in organic materials chemistry in July 2014. Then he joined the group of Professor Klaus Müllen at the Max Planck Institute for Polymer Research (MPIP) for postdoctoral research. His research interests include organic electronic materials and devices as well as bottom-up synthesis of heteroatom-doped graphene molecules and graphene nanoribbons.

mobilities, making it a promising material for future nanoelectronics. However, the lack of a bandgap hinders the straightforward application of graphene in field-effect transistor (FET) devices.[5] In contrast to infinite graphene with a zero bandgap, structurally confined nanoscale graphene segments, which are called nanographenes or graphene quantum dots (GQDs), show non-zero bandgaps that are mainly governed by their size and edge configurations.[6–8] Whereas "top-down" methods, such as hydrothermal or lithographic "cutting" of graphene, cannot control the resulting structure or size distribution of the nanographenes, "bottom-up" chemical synthesis provides access to monodisperse nanographenes with perfectly defined structures and properties.[7,9,10]

Chemical syntheses of polycyclic aromatic hydrocarbons (PAHs) were pioneered by Scholl[11–13] and Clar[14–16] and further developed throughout the 20th century, as summarized in our previous review article.[9] In particular, after highly efficient synthesis of hexa-*peri*-hexabenzocoronene (*p*-HBC, **2**) was established through the oxidative intramolecular cyclodehydrogenation of hexaphenylbenzene (**1**) (Fig. 1), a wide variety of π-extended PAHs were obtained by employing tailor-made oligophenylenes as precursors.[9] Such PAHs, consisting of sp^2 carbon frameworks extending over 1 nm, can be regarded as the smallest possible nanographenes, or graphene molecules.[10,17] In the last decade, the extended PAHs have thus attracted renewed synthetic interest and more interdisciplinary attention as structurally well-defined graphene molecules with great potential in future applications, such as in nanoelectronics, optoelectronics and spintronics.[18–23]

One-dimensional extension of graphene molecules leads to ribbon-shaped nanographenes with high aspect ratios, which are called graphene nanoribbons (GNRs).[24,25] In this article, we defined GNRs as nanographenes with the aspect ratios of larger

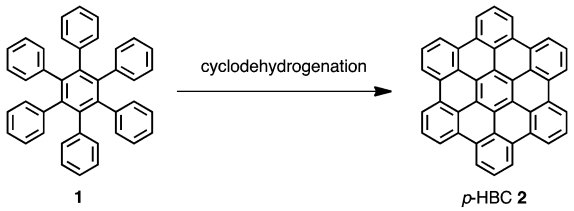

Fig. 1 Synthesis of hexa-*peri*-hexabenzocoronene (*p*-HBC **2**) through intramolecular oxidative cyclodehydrogenation.

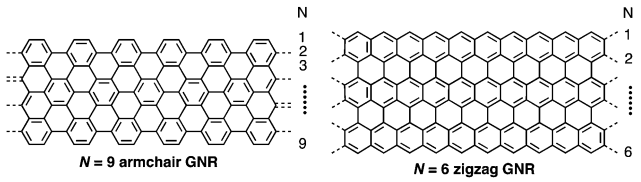

Fig. 2 Structures of *N* = 9 armchair and *N* = 6 zigzag GNRs with the instruction for the counting of number "*N*".

than 10, in order to clearly distinguish them from oblong-shaped graphene molecules.[17] GNRs are categorized by their edge structures, as typically represented by armchair and zigzag configurations (Fig. 2). The width of the armchair and zigzag GNRs is generally defined by the number "*N*" as shown in Fig. 2. The width and the edge structure of the GNRs critically define their physical properties.[26] GNRs with zigzag edge structures are predicted to show localized edge states that can be spin-polarized, which might allow their application to spintronic devices such as spin valve.[27–30] On the other hand, armchair-edge GNRs have non-magnetic semiconducting properties with relatively larger bandgaps, which increase as their

Xinliang Feng

Xinliang Feng, after obtaining his Master's degree in organic chemistry from Shanghai Jiao Tong University in March 2004, joined the group of Prof. K. Müllen at the Max Planck Institute for Polymer Research (MPIP) and obtained his PhD in April 2008. He became a group leader at MPIP in December 2007. Since June 2010, he has been a professor at Shanghai Jiao Tong University and became a distinguished group leader at MPIP in 2012. In August 2014, he became a chair professor at Dresden University of Technology. His current scientific interests include graphene, two-dimensional nanomaterials, organic conjugated materials, and carbon-rich molecules and materials for electronic and energy-related applications.

Klaus Müllen

Klaus Müllen received his PhD in 1972 at the University of Basel (Professor F. Garson) after completing his Diploma in Chemistry at the University of Cologne (Professor E. Vogel) in 1969. He pursued postdoctoral research in the group of J. F. M. Oth at ETH Zurich, where he received his habilitation in 1977 and was appointed a Privatdozent. In 1979, he became a Professor in Organic Chemistry at the University of Cologne and accepted an offer of a chair in Organic Chemistry at the University of Mainz in 1983. In 1989, he became a scientific member of the Max Planck Society and has been the director of the Synthetic Chemistry Department at the Max Planck Institute for Polymer Research. He served as President of the German Chemical Society for two years, beginning January 2008. His current research focuses on synthetic macromolecular chemistry, supramolecular chemistry, and materials science.

width decreases.[26] The armchair GNRs are also predicted to possess high charge-carrier mobilities, which paves the way toward logic applications.[24,31]

The preparation of GNRs has primarily been conducted using "top-down" methods, such as lithographic cutting of graphene sheets[32–34] and unzipping of carbon nanotubes.[35,36] FET devices based on GNRs have been demonstrated, suggesting their considerable potential as emerging semiconductor materials. However, such "top-down" methods are incapable of precise structural control, leading to GNRs with ill-defined widths and edge structures. To reliably tune the (opto-)electronic and spintronic properties of the GNRs, it is imperative to control their structures with atomic precision, which can be achieved by employing the "bottom-up" strategy based on organic synthesis.

The solution-synthesis protocol developed for the preparation of graphene molecules can be successfully applied to longitudinally extended polymeric systems, which enables the formation of structurally well-defined GNRs, in stark contrast to the "top-down" fabricated GNRs with "random" structures.[17,25] A variety of rationally designed polyphenylene precursors have thus been "graphitized" through intramolecular cyclodehydrogenation to provide a number of GNRs with different widths, edge structures and heteroatom doping. Furthermore, in 2010, direct growth of structurally perfect GNRs was achieved on metal surfaces under ultrahigh vacuum (UHV) conditions.[37] Whereas the majority of solution-synthesized GNRs have limited solubility and thus cannot be microscopically investigated, the surface-synthesis protocol allowed *in situ* visualization of the entire GNR formation process with atomic resolution using scanning tunneling microscopy (STM). This complementary synthetic protocol under UHV conditions enabled the synthesis and direct characterization of unprecedented GNR structures that have been unattainable through solution synthesis, including nitrogen-doped GNRs. Furthermore, GNR heterojunctions have experimentally been demonstrated, featuring semiconductor heterostructures with a straddling gap (type I) and a staggered gap (type II).[38,39]

Comprehensive reviews on the bottom-up chemical syntheses of graphene molecules[9,20,23,40–48] and GNRs have been reported.[17,25] Thus, in this review, we focus on the most recent advances in the field. In particular, we first discuss the progress in the synthesis of graphene molecules in four aspects: (1) newly developed, "non-conventional" synthetic methods for graphene molecules, (2) "defective" graphene molecules, involving embedded seven- or eight-membered rings, (3) heteroatom doping of graphene molecules at defined positions and (4) chemical modification of the edges of graphene molecules without prior functionalization. The syntheses and derivatizations of open-shell graphene molecules,[23,46,49–53] contorted PAHs,[20] fullerene fragments,[54–57] acenes,[46,58–61] rylenes,[62,63] helicenes,[64–68] and truxenes[69,70] have been extensively reviewed very recently and are therefore not included in this article. In the second section, the latest developments in the bottom-up synthesis of GNRs from molecular precursors are summarized, focusing on (1) solution-mediated and (2) surface-assisted synthesis of structurally well-defined GNRs and their characterization. Additionally, (3) formation of GNR confined in carbon nanotubes is also described. We have recently published a personal account article, describing our own contributions over the last decade to the development of the GNR synthesis.[25] In the current review article, we provide an overview of the recent advancements in this field, featuring the results that are not covered in the previous article.

II. Synthesis of graphene molecules

Non-conventional approaches for nanographene synthesis

Over the past two decades, concise, high-yielding and scalable synthetic methods have been developed for synthesizing graphene molecules.[9,40] These methods are typically based on intramolecular oxidative cyclodehydrogenation, namely the Scholl reaction,[11,71] of rationally designed oligophenylene precursors (Fig. 1). A wide variety of graphene molecules have thus been synthesized, with different sizes, symmetries and edge structures. Large oligophenylene precursors have conventionally been prepared through cyclotrimerization of diphenylacetylene derivatives or through a combination of substitution and metal-catalysed coupling reactions as well as Diels–Alder cycloaddition of alkyne and tetraphenylcyclopentadienone derivatives.[9,40,72,73] The oxidative cyclodehydrogenation can be performed with a variety of oxidants and Lewis acids,[71] including $Cu(OTf)_2/AlCl_3$,[74] $FeCl_3$,[75] $MoCl_5$,[76] 2,3-dichloro-5,6-dicyano-1,4-benzoquinone (DDQ)/Brønsted or Lewis acid,[77] and [bis(trifluoroacetoxy)iodo]-benzene (PIFA)/$BF_3{\cdot}Et_2O$.[78]

Nevertheless, the scopes of these synthetic methods have been limited by several factors, including incomplete "graphitization,"[79] chlorination[74] and unexpected structural rearrangements[80–83] during the Scholl reaction. Furthermore, oligophenylene precursors, corresponding to the desired graphene molecules, were often inaccessible in the conventional manner. This renders it essential to develop new, "non-conventional" methods for the synthesis of nanographene, which enables preparation of graphene molecules with tailorable (opto-)electronic properties.

In 2013, Dichtel *et al.* reported the synthesis of dibenzo-fused *p*-HBC **6a** *via* sequential benzannulation and cyclodehydrogenation (Fig. 3).[84] Readily accessible di(arylethynyl)-benzene derivatives **3** could be benzannulated by treatment with 2-(phenylethynyl)benzaldehyde, $Cu(OTf)_2$, and CF_3CO_2H to afford precursors **4** in excellent yields, despite the high steric congestion. Interestingly, the following cyclodehydrogenation of **4a** could be performed in a controlled manner, selectively yielding partially fused product **5a** in a shorter reaction time, *i.e.*, ~20 min. An extended reaction time of 240 min led to completely fused graphene molecule **6a** (C50) with 50 sp^2 carbon atoms in the aromatic core (Fig. 3). Formation of graphene molecule **6b** was not observed, probably because of the high steric hindrance caused by the additional *t*Bu groups, affording partially fused **5b** as the final product.

Partially fused PAHs **5** have distinct non-planar structures with a theoretically estimated dihedral torsion angle of 56°. Notably, PAH **5b** exhibited enhanced visible absorption

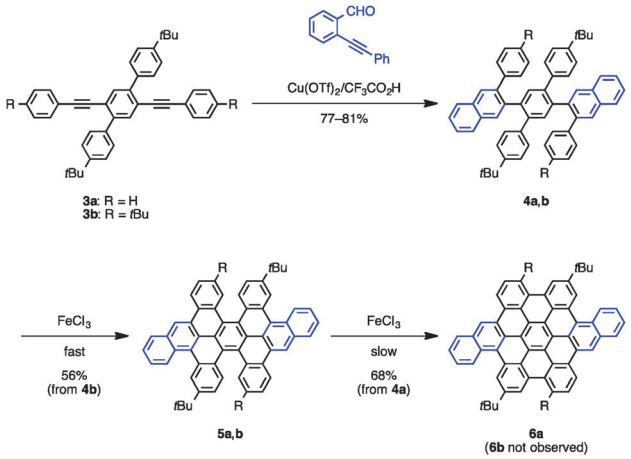

Fig. 3 Syntheses of partially fused PAHs **5** and fully fused graphene molecule **6a** *via* benzannulation and cyclodehydrogenation.

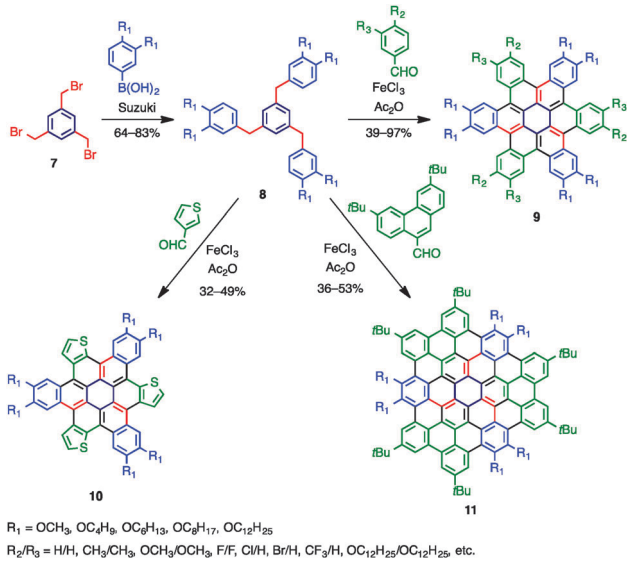

Fig. 4 Facile two-step synthetic route for obtaining C_3 symmetrical *c*-HBC **9**, TBTTC **10** and graphene molecule **11**.

compared with that of fully fused graphene molecule **6a**, with an optical gap of 2.32 eV derived from its UV-Vis absorption spectrum. This value was smaller than the 2.53 eV optical gap of fully fused molecule **6a**, suggesting that the structural non-planarity has an effect on the (opto-)electronic properties of graphene molecules.[85]

This synthetic protocol can be applied to other (arylethynyl)-benzene derivatives,[86] providing potential access to previously unavailable graphene molecules, including contorted species with open bonds at selective positions. Furthermore, the benzannulation strategy has proven to be also effective for poly(phenylene ethynylene)s to yield sterically congested polymers with diarylnaphthalene units,[87] which might serve as precursors for GNRs.

In 2014, Wei and his colleagues developed an elegant two-step synthetic route for obtaining C_3 symmetrically substituted hexa-*cata*-hexabenzocoronenes (*c*-HBCs) **9**, which had been unobtainable through existing methods (Fig. 4).[88] Starting from 1,3,5-tri(bromomethyl)-benzene (**7**), 1,3,5-tribenzylbenzene derivatives (TBBs, **8**) were prepared *via* three-fold Suzuki coupling with phenylboronic acid derivatives. Subsequently, TBBs **8** were reacted with three equivalents of benzaldehyde building blocks under the presence of $FeCl_3$ and acetic anhydride as oxidant/Lewis acid and dehydrating agent, respectively. Remarkably, *c*-HBCs **9** could be obtained in one pot, where a sequence of Friedel–Crafts hydroarylation, intramolecular alkylation, dehydrogenative aromatization, and intramolecular cyclodehydrogenation occurred. By using thienaldehyde instead of benzaldehyde, this synthetic method provided access to *sym*-tribenzotetrathieno-coronenes (TBTTC, **10**), which had been sought after previous syntheses of dibenzotetrathienocoronene (DBTTC)[89,90] and hexathienocoronene (HTC)[91,92] (see Fig. 12). Moreover, phenanthraldehyde could be employed in this protocol to obtain unprecedented C_3 symmetrical graphene molecule **11** with 72 sp^2 carbon atoms in the aromatic core (Fig. 4).

The use of aryne chemistry is also a convenient method for the synthesis of PAHs, involving [4+2] or [2+2+2] cycloadditions.[45,93] In particular, Perez, Guitian, Peña, and co-workers have demonstrated that the palladium-catalysed cyclotrimerization of arynes enables very efficient preparation of triphenylene[94] and a variety of its extended derivatives,[93] including hexabenzo[*a*,*c*,*g*,*i*,*m*,*o*]triphenylene (C42),[95] hexabenzo[*a*,*c*,*k*,*m*,*u*,*w*]trinaphthylene (C54)[96] and hexabenzo[*a*,*c*,*o*,*q*,c_1,e_1]trianthrycene (C66).[97] By further advancing this method, they recently developed a simple synthetic protocol for C_3 symmetrical PAH **17** (C78), starting from bisbenzyne precursor **12** and perylene (**14**) (Fig. 5).[98] Perylene (**14**) was first reacted with aryne **13**, which was generated *in situ* from **12** by treatment with CsF, providing triflate **15** *via* a Diels–Alder cycloaddition. With careful optimization of the reaction temperature and solvent, triflate **15** could be selectively precipitated from the reaction mixture, without further formation of aryne **16**. Under the presence of CsF and a catalytic amount of $[Pd_2(dba)_3]$ (dba = dibenzylideneacetone), triflate **15** was successfully converted to PAH **17** through the palladium-catalysed cyclotrimerization of the *in situ* generated aryne **16**. PAH **17** could be sublimed onto a bilayer of NaCl on Cu(111), and high-resolution atomic

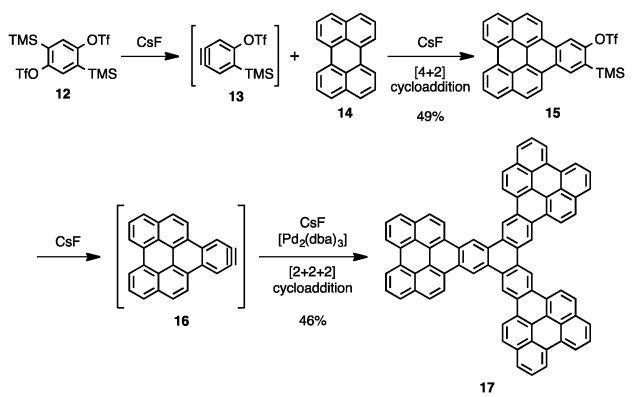

Fig. 5 Synthesis of PAH **17** (C78) through two-step cycloadditions of arynes.

force microscopy (AFM) and STM analyses revealed its molecular structure and orbitals with atomic resolution.

Although syntheses *via* cyclotrimerization of arynes often require multi-step preparation of aryne precursors, cyclotrimerization of *o*-dibromoarenes through Yamamoto coupling can serve as a complementary approach.[99] The Yamamoto conditions can also tolerate silyl groups, which are unstable in the presence of fluoride used for the *in situ* generation of arynes. In 2014, Bunz and co-workers employed this approach of Yamamoto coupling to synthesize unprecedented large starphenes, *i.e.*, trideca-starphene **19** (C54) and hexadeca-starphenes **21** (C66) from dibromotetracene **18** and dibromopentacene **20**, respectively (Fig. 6).[100] Triisopropylsilyl (TIPS)-ethynyl groups were successfully installed on starphenes **19** and **21**, which made them highly soluble in organic solvents, thereby allowing their characterization using NMR and X-ray crystallography. The optical gaps of starphenes **19** and **21** were estimated from their UV-Vis absorption spectra to be 2.29 and 1.76 eV, respectively, which were approximately 0.2 eV smaller than those of linear precursors **18** and **20**.

In addition to the palladium-catalysed [2+2+2] cycloaddition and nickel-mediated Yamamoto coupling, other metal-catalysed reactions are also very useful for constructing graphene molecules.[56,101–103] For instance, palladium-catalysed C–H arylation has been widely used for the preparation of non-planar PAHs incorporating five-membered rings,[56] and palladium-catalysed double cross coupling can extend 1,2-dibromoarenes with 9-stannafluorenes, leading to various triphenylene derivatives.[101] Amsharov *et al.* developed an Al_2O_3-mediated C–H arylation of fluoroarenes *via* C–F activation, allowing the unconventional use of C–F bonds for the intramolecular aryl–aryl coupling of PAHs, for example, to obtain PAH **23** (C46) from fluoroarene **22** (Fig. 7).[104,105]

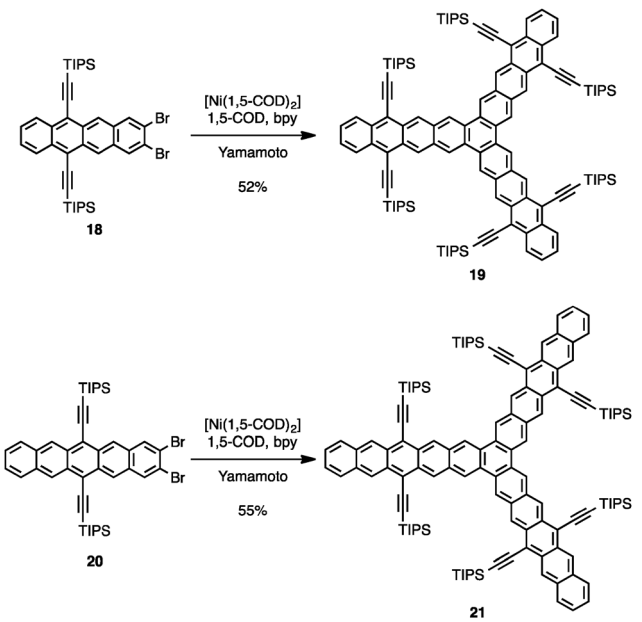

Fig. 6 Syntheses of trideca-starphene **19** and hexadeca-starphenes **21** from dibromotetracene **18** and dibromopentacene **20**, respectively, through Yamamoto coupling.

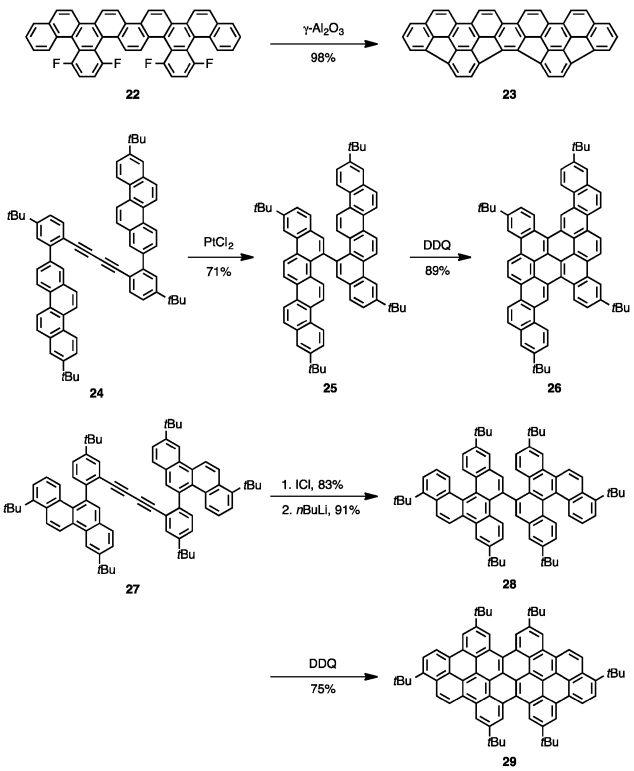

Fig. 7 Syntheses of PAH **23** through Al_2O_3-mediated C–H arylation and of graphene molecules **26** and **29** *via* platinum-catalysed and ICl-mediated cycloaromatization, respectively.

Furthermore, ruthenium- or platinum-catalysed electrophilic cycloaromatization of *ortho*-alkynylated biaryls is a versatile method to form phenanthrene structures, as represented by the conversion of precursor **24** to [6]phenacene **25**, which enabled the synthesis of graphene molecule **26** (C52) through subsequent cyclodehydrogenation (Fig. 7).[56,106–108] Here, ICl-mediated cycloaromatization of *ortho*-alkynylated biaryls can serve as a metal-free alternative method for obtaining halogenated phenacenes, which can be directly used for further coupling reactions or dehalogenated by simple treatment with *n*-butyllithium.[103,106,107,109,110] Although the platinum-catalysed cycloaromatization of precursor **27** was unsuccessful, the use of ICl allowed conversion of **27** to [4]phenacene **28**, followed by graphitization to graphene molecule **29** (C52) (Fig. 7).[106] Further details regarding such metal-catalysed or metal-mediated reactions can be found in recent review articles.[56,101–103,111,112]

Graphene molecules with seven- or eight-membered rings

As two-dimensionally confined structures of graphene, nanographenes, in principle, consist of only six-membered rings. However, microscopy studies have revealed that graphene also contains rings of other sizes, including five-, seven- and eight-membered rings, as defects, particularly at the grain boundaries of graphene sheets grown by chemical vapour deposition (CVD).[113–117] Therefore, extended PAHs containing non-six-membered rings can indeed be considered as graphene molecules, which allow model studies of ''defective'' graphene and may also find

applications in (opto-)electronics. PAHs with five-membered rings have been extensively synthesized and investigated as fullerene fragments and their derivatives following the pioneering works by Scott *et al.*[44,54–57,102,118] However, there are only scarce examples of graphene molecules containing seven- or eight-membered rings.

PAHs with a central *n*-membered ring that is completely surrounded by fused benzenoid rings are called [*n*]circulenes, based on the definition by Wynberg.[119–121] According to this definition, corannulene and coronene are [5]circulene and [6]circulene, respectively. Moreover, [7]circulene and [8]circulene can be regarded as graphene molecules containing seven- and eight-membered rings, respectively. [7]Circulene was first synthesized by Yamamoto and Nakazaki *et al.* in 1983,[122] followed by [7.7]circulene in 1991, which incorporated two seven-membered rings.[123] Nevertheless, graphene molecules with embedded seven-membered rings, other than the circulenes, had remained elusive.

In 2012, Miao *et al.* reported a curved graphene molecule **31** with an embedded seven-membered ring (Fig. 8), which is π-isoelectronic to *p*-HBC **2** (C42).[124] The synthesis consisted of the oxidative cyclodehydrogenation of hexaphenylbenzene-based precursor **30**, which was prepared *via* the Diels–Alder cycloaddition of a tetraphenylcyclopentadienone derivative and an aryne generated *in situ* from 10-bromo-5*H*-dibenzo[*a*,*d*]-cycloheptene (Fig. 8). Introduction of alkoxyl groups at *ortho* or *para* positions to the reaction sites was found to be crucial for achieving the complete cyclodehydrogenation process; otherwise, a mixture of inseparable products was obtained. In a follow-up report in 2015, they synthesized two new aromatic saddles, $C_{70}H_{26}$ (**34a,b**) and $C_{70}H_{30}$ (**36a,b**), with two embedded heptagons.[125] The synthesis was carried out through saddle-shaped diketones (**32a,b**) as the key precursors, bearing two tropone subunits incorporated in the well-known framework of *p*-HBC. These aromatic saddles **34** and **36** were successfully obtained by π-extension on the carbonyl groups of precursor **32** and further oxidative cyclodehydrogenation. The saddle-shaped structures of these graphene molecules were unambiguously characterized by single-crystal X-ray analysis.

In 2013, Durola and co-workers conducted oxidative cyclodehydrogenation of sterically congested precursor **37** and unexpectedly obtained graphene molecule **38** (C66) as a major product (Fig. 8), whose structure was confirmed by X-ray crystallographic analysis.[126] Although the expected C_3 symmetric graphene molecule was not obtained due to the rearrangement during the Scholl reaction, graphene molecule **38** is one of the rare examples with an embedded seven-membered ring. This result provides further insights into the rearrangements or migration of aryl groups in the Scholl reaction, which still remain elusive.

In 2013, Scott, Itami, and co-workers made major progress, achieving concise, two-step synthesis of grossly warped graphene molecule **42** (C80) with five embedded seven-membered rings and one five-membered ring at the centre (Fig. 9).[127] Starting from corannulene (**39**), precursors **40** and **41** were obtained by palladium-catalysed direct C–H arylation with arylboroxins, using *o*-chloranil as an oxidant.[128,129] Remarkably, the

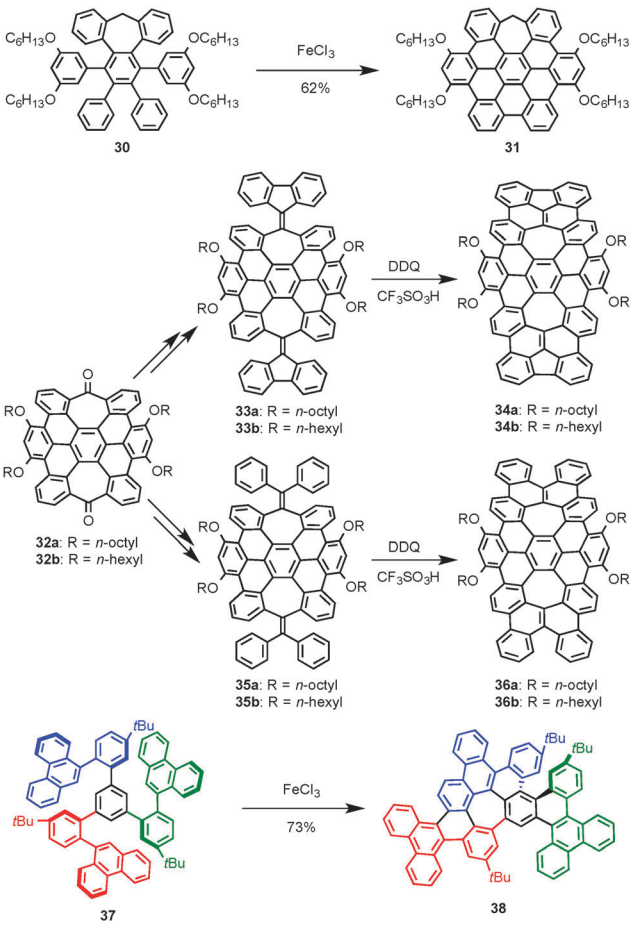

Fig. 8 Syntheses of graphene molecules **31**, **34**, **36** and **38** with embedded seven-membered rings through cyclodehydrogenation.

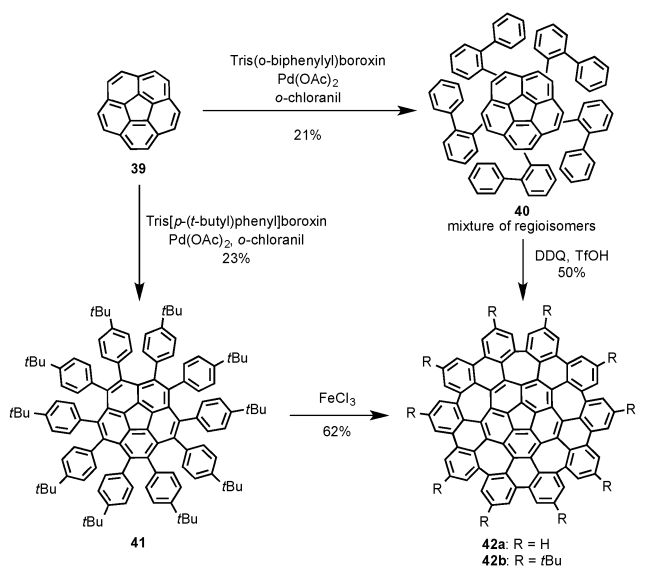

Fig. 9 Synthesis of grossly warped graphene molecules **42** through C–H arylation and cyclodehydrogenation of corannulene (**39**).

intramolecular cyclisation of precursors **40** and **41** efficiently provided grossly warped graphene molecule **42** in good yields, overcoming the high steric demand to form five distorted seven-membered rings. Because of its highly non-planar structure, graphene molecule **42** showed good solubility in common organic solvents, and, astonishingly, graphene molecule **42b** with *tert*-butyl groups could be dissolved even in hexane. Graphene molecule **42** was comprehensively characterized spectroscopically, and X-ray crystallographic analysis revealed that **42** possessed a unique double-concave structure. Although the oxidative cyclodehydrogenation has been employed almost exclusively for preparing of planar graphene molecules, the above-mentioned recent results clearly demonstrated that it is also a very powerful method for synthesizing non-planar graphene molecules.

Whereas [7]circulene was synthesized in 1983,[122] [8]circulene had not been achieved until recently, probably because of its highly strained and instable structure.[130] The first synthetic attempt was reported in 1976 by Wennerström *et al.*, but photocyclisation of [2,2](3,6)phenanthrenophanediene in the final step did not afford the [8]circulene, presumably owing to the high steric demand.[131] In 2013, Wu and co-workers reported the first synthesis of *peri*-substituted [8]circulene **44** through four-fold palladium-catalysed annulations of tetraiodo-substituted tetraphenylene **43** with diarylethynes (Fig. 10).[132] Octaaryl-[8]circulene **44** could be obtained in remarkable 60–75% yields, corresponding to ~88–93% for each annulation step, allowing the preparation of several hundred milligrams of **44**. [8]Circulene **44** was unambiguously characterized through NMR and X-ray crystallographic analyses, which revealed its non-planar saddle-like structure.

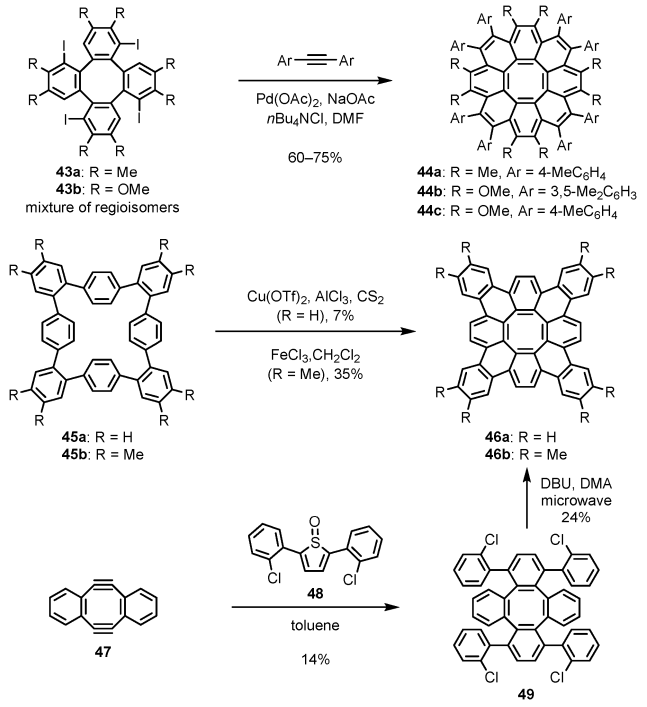

Fig. 10 Syntheses of [8]circulene **44** through palladium-catalysed annulation and of tetrabenzo[8]circulene **46** through oxidative cyclodehydrogenation or a sequence of Diels–Alder cycloaddition and palladium-catalysed C–H arylation. DBU: 1,8-diaza-bicycloundec-7-ene; DMA: *N*,*N*-dimethylacetamide.

Later in the same year, Sakamoto and Suzuki reported the synthesis of tetrabenzo[8]circulene **46** *via* oxidative cyclodehydrogenation (Fig. 10).[133] Cycloocta-*o*,*p*,*o*,*p*,*o*,*p*,*o*,*p*-phenylene **45a** was prepared as a precursor through Suzuki coupling of *o*-terphenylboronic ester and *o*-dibromobenzene. Precursor **45a** was subsequently subjected to cyclodehydrogenation with $Cu(OTf)_2$ and $AlCl_3$, affording tetrabenzo[8]circulene **46a** in 7% yield. Because the intermolecular coupling to form a dimeric byproduct was found to be one reason for the low yield, precursor **45b** with eight methyl groups was subsequently prepared. Oxidative cyclodehydrogenation of precursor **45b** with $FeCl_3$ provided octamethyl-tetrabenzo[8]circulene **46b** in an improved (35%) yield. X-ray crystallographic analysis of tetrabenzo[8]circulene **46a** showed its deep saddle structure with two S_4-symmetrical conformers, which were twisted from the D_{2d}-symmetrical ground-state structure revealed by density functional theory (DFT) calculations. This observation provided evidence for the theoretically predicted pseudorotation of tetrabenzo[8]circulene **46** *via* a non-planar transition state.

At almost the same time, Whalley and co-workers developed another synthetic route for tetrabenzo[8]circulene **46a** based on a sequence of Diels–Alder cycloaddition and palladium-catalysed C–H arylation (Fig. 10).[134] In the first step, dibenzocyclooctadiyne **47** was subjected to two-fold Diels–Alder reactions with 2,5-diarylthiophene-1-oxide **48** to afford tetrabenzocyclooctane precursor **49**. Interestingly, Diels–Alder reactions using 2,5-diphenylfuran or 2,5-diphenylthiophene dioxide instead of **48** required higher temperatures, resulting in the decomposition of dibenzocyclooctadiyne **47**. This result indicated the high potential of thiophene-1-oxides as the dienes in the Diels–Alder reactions although they have rarely been used for this purpose. Subsequently, the palladium-catalysed C–H arylation of precursor **49** afforded tetrabenzo[8]circulene **46a** in 24% yield. Because of its full benzenoid structure, tetrabenzo[8]circulene **46** exhibited high stability, in contrast to the parent [8]circulene, without any deterioration under ambient conditions over five months or at 100 °C for 24 h.

Apart from the [8]circulene derivatives, there are scarce examples of graphene molecules with embedded eight-membered rings. In 2014, our group reported the synthesis of biphenylene-based PAH **51**, incorporating one eight-membered and one four-membered rings, through oxidative cyclodehydrogenation of octaarylbiphenylene **50** (Fig. 11).[135] The cyclodehydrogenation did not proceed further, probably because of the high steric demand, selectively providing PAH **51** in 90% yield. The UV-Vis absorption and emission spectra of PAH **51** revealed its relatively large optical bandgap of ~2.8 eV and an emission at 552 nm, respectively. A large Stokes shift of 4000 cm^{-1} was observed, which indicated partial planarization of PAH **51** in the excited state.

Heteroatom-doped graphene molecules

Heteroatom-doped graphene is a new class of materials that possess properties and functions different from those of the

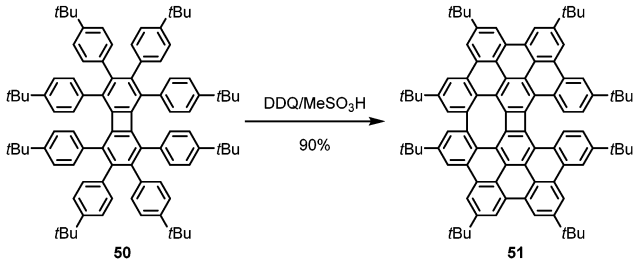

Fig. 11 Synthesis of biphenylene-based PAH **51**, containing one eight-membered ring and one four-membered ring, *via* cyclodehydrogenation of octaarylbiphenylene **50**.

parent graphene.[136–138] However, the heteroatom doping of graphene sheets with precise structural control has not been achieved, hindering studies of structure–property relationships at the atomic or molecular level. By contrast, bottom-up organic synthesis can provide structurally defined heteroatom-doped graphene fragments with perfect control not only of the size, periphery and substituent, but also of the doping concentration and position. Although a wide variety of heteroatom-doped structures have been developed for small PAHs, until recently there had been only a few examples for expanded PAHs.[41,60,139–141]

As typical examples of nitrogen (N)-doped graphene molecules, we developed a series of pyrrole-fused azacoronenes **52–55** (Fig. 12), together with Takase, Nishinaga and their colleagues, through the oxidative cyclodehydrogenation of corresponding hexaarylbenzenes.[142,143] These PAHs incorporating electron-rich pyrrole-type nitrogens exhibited up to four reversible oxidation processes in the electrochemical measurements. They were also easily oxidized by chemical oxidants, *e.g.*, $SbCl_5$, to generate radical cations and dications.

The stepwise replacement of pyrrole rings with dialkoxybenzenes significantly changed their optical and electronic properties in both neutral and oxidized states. For example, the emission colours of these compounds changed from red to green as the number of pyrrole rings decreased from six (**52**) to three (**55**) (Fig. 12). The quinoidal resonance structures of $\mathbf{52}^{2+}$ and $\mathbf{53}^{2+}$ stabilized these dication species, inducing higher oxidation potentials in the next step from dication to trication states, which was not observed for $\mathbf{54}^{2+}$ and $\mathbf{55}^{2+}$. In the dication states, hexaazacoronene $\mathbf{52}^{2+}$ and pentaazacoronene $\mathbf{53}^{2+}$ exhibited a closed-shell character. On the other hand, an open-shell character was theoretically predicted for tetraazacoronene $\mathbf{54}^{2+}$ and triazacoronene $\mathbf{55}^{2+}$. The introduction of dialkoxybenzenes instead of pyrrole rings prohibited the charge/spin delocalization in the π-system, which resulted in "weakly interacting" spins with an open-shell character. In addition, small S_1–T_1 energy gaps (<0.36 eV) were observed in this family of compounds, which is very interesting, particularly in the field of molecular photonics, considering the possibility of thermally activated T_1 to S_1 intersystem crossing.[144]

In 2014, Stępień and co-workers explored a new type of expanded hexapyrrolohexaazacoronenes **56** and **57** with interrupted peripheral conjugation, by introducing saturated methylene bridges (Fig. 12).[145] These molecules can also be regarded as the first examples

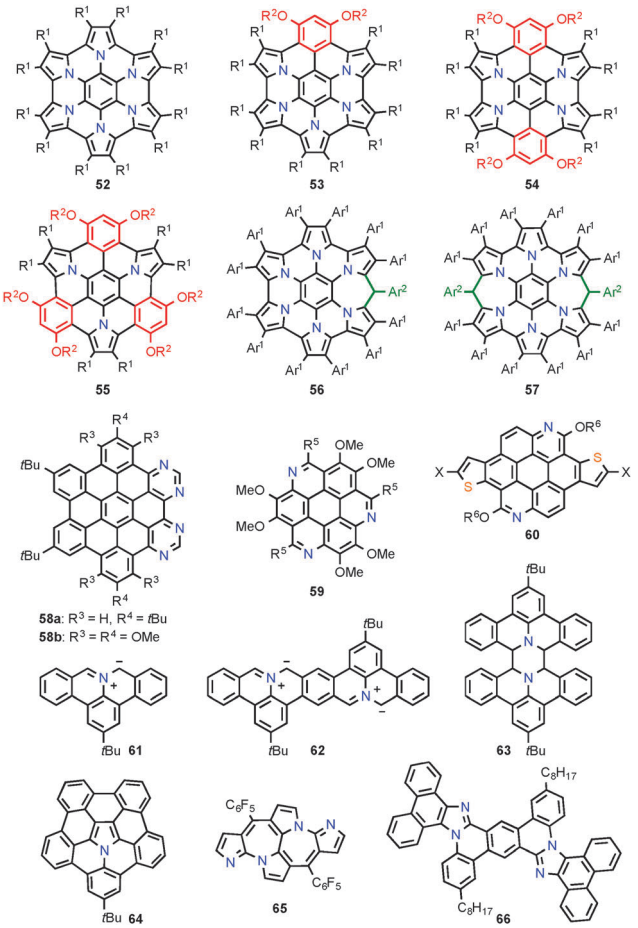

Fig. 12 Representative examples of N-doped PAHs. R^1: H or 4-trifluoromethylphenyl; R^2: methyl, *n*-butyl or *n*-dodecyl; Ar^1: *p*-butoxyphenyl; Ar^2: *p*-nitrophenyl; R^5: phenyl, 4-methoxyphenyl, 4-bromophenyl, methyl, hexyl, *etc.*; R^6: 2-ethylhexyl or 2-decyltetradecyl; X: H, Br, trimethylstannyl, *etc.*

of N-doped graphene molecules with embedded seven-membered rings. The synthesis was conducted from substituted hexapyrrolylbenzenes in a two-step condensation–aromatization sequence, *i.e.*, a Lewis acid-catalysed bridging with *p*-nitrobenzaldehyde followed by oxidative cyclodehydrogenation. Notably, the peripheral bridges could be aromatized through oxidative dehydrogenation, and subsequent nucleophilic additions proceeded in a perfectly stereospecific manner, allowing functionalization with a variety of substituents. These new azacoronenes with methylene bridges exhibited easily accessible higher oxidation states. Remarkably, contrary to the cases of **52–55**, a tetracationic species $\mathbf{57}^{4+}$ could be chemically generated by oxidation with $SbCl_5$, which was presumably enabled by the disrupted peripheral conjugation.

In contrast to the electron-rich pyrrole-fused graphene molecules, incorporation of imine-type nitrogen in the PAH framework by fusing pyridine or pyrimidine rings creates electron-deficient N-doped graphene molecules. In 2002, Draper *et al.* reported the first example of such a molecule, namely, N-doped *p*-HBC **58a** (Fig. 12), through the oxidative dehydrogenation of a corresponding pyrimidine-incorporated hexaarylbenzene precursor.[146]

N-doped *p*-HBC **58a** served as a versatile ligand for metal (*e.g.*, Pd^{II} and Ru^{II}) complexes.[147] The photophysical properties of N-doped *p*-HBC **58a** were demonstrated to be effectively modulated by metal coordination.

In 2014, Draper *et al.* performed methoxy functionalization on the periphery to obtain N-doped *p*-HBC **58b** and found that the cyclodehydrogenation process was promoted by incorporating electron-donating methoxy groups.[148] The photophysical and electronic properties were profoundly affected by the methoxy substitution. Furthermore, the X-ray crystal structure of **58b** revealed that the intermolecular hydrogen bonds involving methoxy groups and nitrogen atoms assist the molecules to arrange in a head-to-tail manner in the columnar stack.

The family of PAHs doped with imine-type nitrogens also includes azacoronene derivatives. For example, 1,5,9-triazacoronene **59** was synthesized by Wei *et al.* with a threefold Pictet–Spengler reaction as the key step (Fig. 12).[149] These compounds exhibited an electron-deficient nature compared to the all-carbon analogue. Recently, Liu *et al.* reported a novel thiophene-fused azacoronene **60**, featuring two imine-type nitrogens on the skeleton.[150] Azacoronene **60** bearing bromo or trimethylstannyl groups could be further functionalized through Stille coupling, which also allowed incorporation of **60** into conjugated polymers. Azacoronene **60** with two fused thiophene rings was relatively electron-rich and showed hole mobilities of up to 0.028 $cm^2\ V^{-1}\ s^{-1}$ in FET devices. Furthermore, conjugated polymers incorporating azacoronene **60** functioned as the donor material in organic photovoltaic devices, which exhibited a high open-circuit voltage of 0.89 V and a power conversion efficiency (PCE) of 4.8%.

In 2014, we reported the synthesis of dibenzo-9*a*-azaphenalene (**61**), which features a N-doped zigzag-edge structure (Fig. 12).[151] With **61** as the basic unit, its dimer **62** was also successfully synthesized, suggesting the possibility of further lateral extension toward N-doped zigzag-edge GNRs. Dibenzoazaphenalenes **61** and **62** are featured with azomethine ylide structures, showing extremely high chemical reactivity, and thus they were generated only under inert conditions. Azomethine ylide **61** could be employed in 1,3-dipolar cycloaddition reactions with various dipolarophiles, providing a unique pathway to N-doped PAHs with fused pyrrole rings.[152] Nozaki *et al.* found that **61** can also react with fullerene C_{60} to form an adduct.[153]

Furthermore, generation of **61** at a high temperature provided self-dimerization product **63** in 51% yield, which might serve as a precursor for an unprecedented *p*-HBC with two nitrogen atoms inside the aromatic core.[151] In 2015, Ito and Nozaki *et al.* achieved an unprecedented synthesis of 6b^2-azapentabenzo[*bc*,*ef*,*hi*,*kl*,*no*]-corannulene **64** based on the 1,3-dipolar cycloaddition of azomethine ylide **61** with 2,2′,6-trichlorodiphenylacetylene, followed by three-fold Pd-catalysed cyclisation (Fig. 12).[154] N-doped corannulene derivative **64** is a rare example of bowl-shaped PAHs with heteroatom doping inside the aromatic framework, and demonstrated distinctly different structural and opto-electronic properties compared to the parent corannulene. These results indicate a high potential of the azomethine ylide chemistry based on **61** and its derivatives for exploring a new class of N-doped PAHs, which cannot be accessed by other synthetic methods.

In 2015, Anand and co-workers reported a metal-assisted cyclodimerization of doubly N-confused dipyrrin into azaheptalene **65**.[155] Single-crystal X-ray analysis revealed the planar structure of **65** with two embedded seven-membered rings. In the same year, Gryko and co-workers reported a photochemical direct arylation method to convert phenanthro[9,10-*d*]-imidazole derivatives with 2-halogenoaryl substituent into phenanthro-[9′,10′:4,5]imidazo[1,2-*f*]-phenanthridines, such as N-doped PAH **66**, in high yields.[156] This reaction occurred without a need of any photosensitizer or base, presumably through the formation of a radical anion as a critical step.

Thiophene-fused PAHs have been extensively explored because of their wide applications in organic electronic devices.[157–159] From the synthetic point of view, several beautiful thiophene-annulated structures have also been developed, such as octathio[8]circulene ("sulflower"),[160] tetrathienoteropyrene,[161] thiophene-fused heptalenes[162] and coranulenes.[163] Here we focus on π-extended PAHs, mainly consisting of hexagonal rings, as sulphur (S)-doped graphene molecules. We synthesized a tribenzothiophene-fused *p*-HBC **67** as the first example of such molecules with embedded thiophene rings (Fig. 13).[164] In 2011, Draper *et al.* reported *p*-HBC **68** with an embedded thiophene ring *via* oxidative cyclodehydrogenation.[165] They could also obtain a dimer of S-doped *p*-HBC **68** through intermolecular oxidative coupling at the thiophene rings, which showed concentration-dependent optical properties governed by the relative orientation between the two S-doped HBC planes.

In addition to these examples based on *p*-HBC, Nuckolls *et al.* developed a synthesis of dibenzotetrathienocoronene (DBTTC) **69**, a thiophene-fused *c*-HBC analogue (Fig. 13).[89,90] The aromatic core of **69** could self-assemble into a columnar superstructure, which merged into a three-dimensional network of supramolecular cables. When the acceptor C_{60} was evaporated

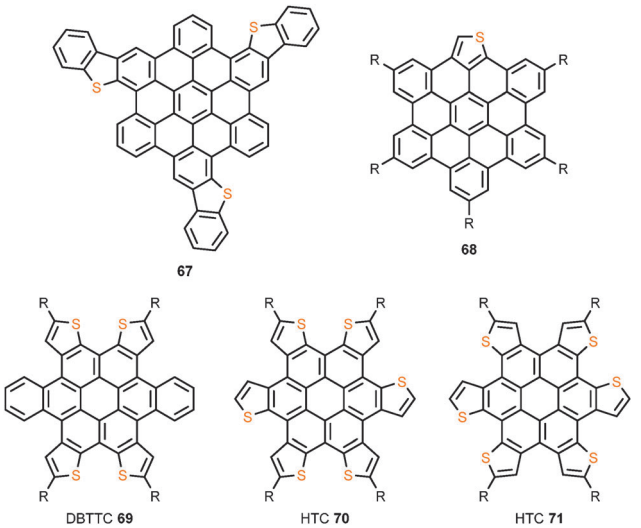

Fig. 13 Examples of S-doped graphene molecules. R represents hydrogen or alkyl substituents.

into this network, a nanostructured p–n bulk heterojunction was formed, providing a PCE of 1.9% in a solar cell device. Furthermore, solution-processed photovoltaic devices of DBTTC **69** and phenyl-C_{70}-butyric acid methyl ester ($PC_{70}BM$) showed a PCE of 2.7%, where a supramolecular complex between **69** and $PC_{70}BM$ was demonstrated to play an important role in the charge separation process.[166]

More recently, we synthesized a class of fully thiophene-annulated coronenes, namely, hexathienocoronenes (HTCs) **70** and **71**, which are stronger electron donors with higher HOMO levels compared to DBTTC **69** (Fig. 13).[91] Based on single-crystal X-ray analysis, HTC **71** adopted an almost planar conformation due to the relatively weak steric congestion of the six peripheral thiophene rings. Columnar stacking was also observed for **71**, providing suitable charge transport channels. The skeleton of HTC **71** was later used to construct a gemini-type amphiphile, which yielded various ordered assemblies in solution, at the liquid–solid interface and in the solid state.[92] Remarkably, the blend of amphiphile **71** and $PC_{60}BM$ exhibited photoconductive properties with a large on/off ratio of 6×10^4. The synthesis of TBTTC **10** by Wei *et al.* (Fig. 4) further enriched the diversity of the family of thiophene-fused *c*-HBC analogues as described above.

Boron (B) atoms have also been incorporated in PAHs, resulting in intriguing properties. Generally, B-containing compounds are unstable toward moisture and oxygen owing to the intrinsic high reactivity of B atoms. Bulky substituents are thus typically required to kinetically protect the Lewis acidic B centre.[167] However, the steric bulkiness prevents intermolecular interactions in the solid state, which is detrimental to charge transport properties. Yamaguchi *et al.* proposed a new strategy for stabilizing tri-coordinated boron-containing π-systems by "structural constraint."[168,169] The planarized skeleton was highly stable and could be handled without any special precautions. Using this strategy, Yamaguchi *et al.* achieved the synthesis of the first example of B-doped graphene molecule **72**, which contained two boron atoms inside the carbon framework (Fig. 14).[170] The key step of the synthesis consisted of oxidative cyclodehydrogenation using $FeCl_3$. The boron atoms had a significant contribution to the molecular orbitals, which induced broad absorption over the entire visible region as well as fluorescence extending to the NIR region. They also demonstrated syntheses of extended triphenylborane **73**[171] and internally B-doped PAH **74** with two fused-thiophene rings and an embedded seven-membered ring (Fig. 14).[169] In 2015, Wagner and co-workers reported a modular synthesis of B-doped PAHs, including 7,14-diborabisanthene **75**.[172] The replacement of the two *meso* carbons of bisanthene with B atoms turned a near-infrared dye into an efficient blue fluorescent compound (**75**) with a high quantum yield of 78%.

Another approach to incorporating B atoms in π-conjugated systems consists of replacing the common CC unit with its isoelectronic BN unit, which has led to a new class of compounds that have properties distinct from those of their carbon analogues but maintain structural similarity.[139–141] The dipolar BN unit has a significant impact on the molecular orbitals, intermolecular interactions and photophysical and redox properties of the π-system, providing a unique strategy for molecular engineering.[173–178] In 2015, Pei *et al.* reviewed the history and progress of BN-substituted PAHs, and proposed that suitable BN-containing PAHs could be used as precursors for the bottom-up construction of BN-doped graphenes with well-defined structures.[139] Here we mainly focus on large BN-embedded π-skeletons, which are model compounds and potential precursors for BN-doped graphenes.

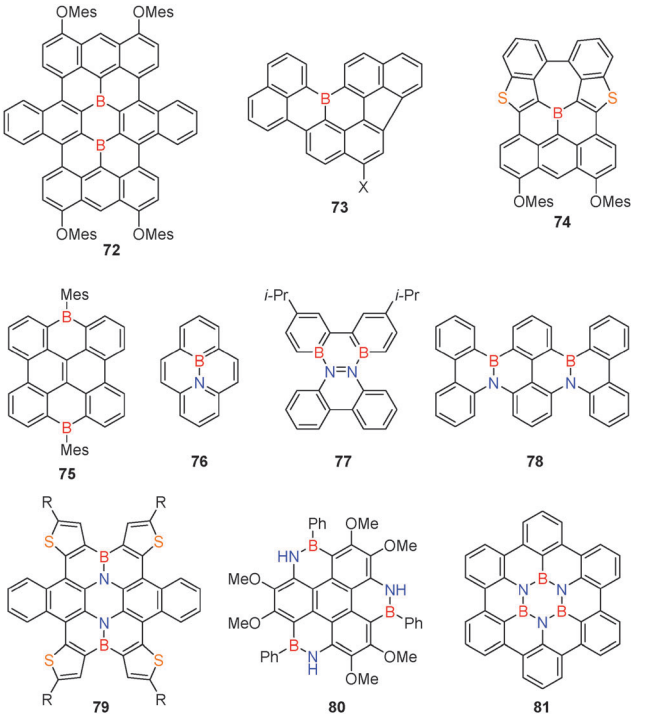

Fig. 14 Examples of B- and BN-doped PAHs. Mes: mesityl; X: H, Br or Ph; R: *n*-butyl or *n*-hexyl.

Piers and co-workers developed a series of BN-embedded PAHs, such as BN-substituted pyrene (**76**)[179] and dibenzo[*g*,*p*]-chrysene (**77**),[180] which raised modern research interest in this field. In 2011, Hatakeyama, Seki and Nakamura *et al.* reported the first step toward extended BN-doped PAHs, demonstrating the synthesis of BN-doped hexabenzotetracene **78** through tandem intramolecular electrophilic arene borylation (Fig. 14).[178] In 2014, Pei *et al.* pioneered a straightforward strategy toward BN-doped graphene molecules by employing azaacenes as a platform for constructing large BN-embedded π-systems.[181] As a proof of concept, π-extended BN heterocoronene derivatives **79** with two BN units were synthesized from 6,13-dihydro-6,13-diazapentacene (Fig. 14). The ring-closure step involved the efficient construction of two B–N bonds and four B–C bonds through an electrophilic borylation method. The introduction of BN units in the skeleton had a pronounced influence on its electronic properties and molecular geometry. The molecules showed a tendency to pack into a columnar structure, which facilitated the formation of one-dimensional micro-ribbons through solution-processed self-assembly. FET devices based on the micro-ribbons exhibited hole mobilities of up to 0.23 $cm^2\ V^{-1}\ s^{-1}$. Photoconductive properties were also observed, indicating the potential application

of BN-embedded graphene molecules for organic photovoltaics. This work also paved a way toward the fabrication of BN-doped graphenes based on the π-extension of BN-containing PAHs.

In 2015, Pei *et al.* and Zhang *et al.* almost simultaneously reported their independent syntheses of C_3-symmetric BN heterocoronene **80** with three BN units (Fig. 14).[182,183] The planar and aromatic structure of **80** was clearly revealed by the single-crystal X-ray analysis and NMR spectroscopy. The UV-Vis absorption and emission spectra of **80** showed blue-shifted peaks compared to those of a similarly alkoxylated coronene,[184] demonstrating an increase of the energy gap as a result of the BN doping.[182] The phenyl groups at the B positions were selectively replaced with hydroxy groups in wet organic solvents, which further increased the energy gap.[183] In the same year, Bettinger *et al.* successfully constructed B_3N_3-doped *p*-HBC **81** by thermolysis of a tris(2-biphenylyl)borazine precursor at 550 °C.[185] The structure was verified by mass spectrometry and infrared and solid-state NMR spectroscopy. B_3N_3-doped *p*-HBC **81** was also sublimated onto Au(111) surfaces for STM characterization, which showed that this molecule lies flat on the surface in a 2D pattern.

Phosphorus (P)-doped graphene molecules are another very interesting class of compounds, considering the remarkable (opto-)electronic properties of phosphole-based materials.[186–188] Nevertheless, there are only a few examples of PAHs with embedded P atoms. In 2011, Hatakeyama and Nakamura *et al.* reported the synthesis of P-doped PAH **82** through the tandem phospha-Friedel–Crafts reaction, demonstrating the extended π-conjugation over the entire molecule (Fig. 15).[189] In 2014, they further extended the synthesis and obtained P-doped PAH **83** with high structural distortion.[190] On the other hand, Réau and co-workers succeeded in the preparation of planar P-doped PAH **84** *via* photocyclisation.[191] Notably, the (opto-)electronic properties of PAH **84** could be starkly modified by utilizing the reactivity of the P centre, *e.g.*, through transformations into thiooxophosphole, oxophosphole and phospholiums, allowing fine-tuning of its energy gap.

Direct edge functionalization of graphene molecules

Although the physical properties of graphene molecules are governed primarily by their aromatic core structures, substituents at their peripheries also play a major role.[21,192] For example, alkyl chains as the substituents can change the solubility and the phase-forming and self-assembly behaviour of graphene molecules, which in turn affect, *e.g.*, the performance of (opto-)electronic devices fabricated with them. By introducing electron-donating or electron-withdrawing groups as substituents, it is also possible to directly modify their (opto-)electronic properties. Moreover, substitution with chemically reactive substituents such as halogens allows further structural functionalization of graphene molecules.

Nevertheless, the introduction of different substituents at the edges of graphene molecules often requires tedious synthetic input, starting from the modification of basic building blocks. Moreover, the scope of substituents that can be introduced is often limited because of their instability or incompatibility under the reaction conditions. For example, the oxidative cyclodehydrogenation could be hampered by increased steric hindrance or modification of the electronic energy levels by the substitution. Therefore, direct edge functionalization of already formed graphene molecules is desirable but yet remains underexplored.

Halogens on the edges of graphene molecules can be converted to cyano groups,[193,194] and be used for various metal-catalysed coupling reactions, such as Sonogashira, Suzuki and Buchwald coupling with terminal alkynes,[195,196] boronic acids/esters[197] and primary/secondary amines,[193,194] respectively. Moreover, alkoxy and ester groups can also be introduced *via* palladium-catalysed coupling reactions.[193] Nevertheless, these methods require the prior introduction of halogens.

In 2013, we reported a very efficient edge chlorination protocol for extended graphene molecules that consists simply of refluxing with an excess amount of iodine monochloride and a catalytic amount of $AlCl_3$ in carbon tetrachloride.[198] Syntheses of a series of perchlorinated graphene molecules, as represented by **85–89**, have thus been achieved in excellent yields, with the number of sp^2 carbon atoms ranging from 42 to 222 (Fig. 16). The electronic energy levels of the graphene molecules were lowered by the edge chlorination, providing an unprecedented class of n-type graphene molecules that function as electron

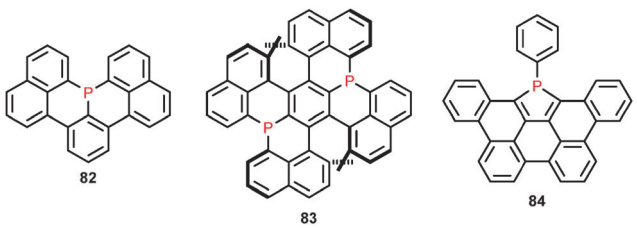

Fig. 15 Examples of P-doped PAHs.

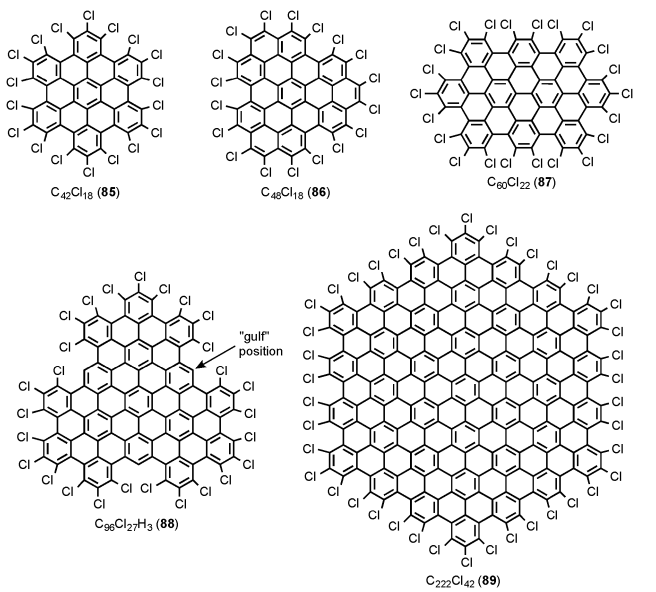

Fig. 16 Examples of edge-chlorinated graphene molecules.

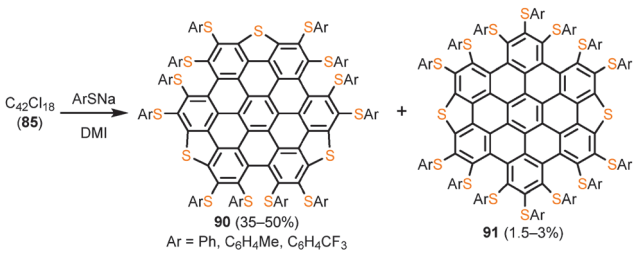

Fig. 17 Synthesis of sulphur-annulated graphene molecules **90** and **91** through the thiolation of perchlorinated HBC **85**. DMI: 1,3-dimethyl-2-imidazolidinone.

transporting materials. The bandgaps of the graphene molecules were also reduced compared to their parent molecules. Furthermore, the planarity of the graphene molecules was distorted by the steric hindrance between the chloro groups densely attached on the peripheral positions, which drastically enhanced their solubility. The increased solubility enabled their liquid-phase characterizations, solution processing and even X-ray single-crystal analysis of unprecedentedly large PAH molecules, including **88** with 96 sp^2 carbons. Interestingly, the crystal structure of **88** showed that the "gulf" position[199] of graphene molecules was not chlorinated (Fig. 16), most likely due to the steric hindrance caused by the two chloro groups installed on the neighbouring positions.

The chloro groups installed at the peripheries of the graphene molecules can be employed for further chemical functionalizations. Based on perchlorinated HBC **85**, we very recently demonstrated edge-thiolation of graphene molecule, which provided unprecedented tri-sulphur-annulated HBC (TSHBC) **90** and di-sulphur-annulated HBC (DSHBC) **91** densely decorated with arylthio groups (Fig. 17).[200] X-ray single-crystal analysis unambiguously demonstrated the structures of HBCs **90** and **91** with embedded thiophene rings, which constitute a new class of S-doped graphene molecules with S-annulated peripheries. The UV-Vis absorption spectrum of TSHBC **90** showed a significant red shift of 100 nm compared to that of parent *p*-HBC **2**, indicating a decrease in the optical bandgap of 0.5 eV. Electrochemical studies of TSHBC **90** revealed three reversible reduction processes, which could be tuned by introducing electron-donating or electron-withdrawing groups on the arylthio substituents.

Shinokubo and co-workers applied the iridium-catalysed direct borylation reaction[201] to *p*-HBC derivatives, such as **92**, providing diborylated *p*-HBC **93** (Fig. 18).[202,203] Starting from diborylated *p*-HBC **93**, they synthesized a variety of *p*-HBC derivatives.[202,204] First, diborylated *p*-HBC **93** was oxidized to dihydroxy-*p*-HBC **94** and then methylated to afford dimethoxy-*p*-HBC **95**. *p*-HBC bistriflate **96** was also prepared from dihydroxy-*p*-HBC **94**, which could be employed for various palladium-catalysed coupling reactions. Alkynyl-substituted *p*-HBC **97** and diamino-*p*-HBC **98** could thus be obtained through Sonogashira coupling and Buchwald–Hartwig amination, respectively. Furthermore, *p*-HBC bistriflate **96** could also be cyanated to dicyano-*p*-HBC **99** based on a cyanation protocol reported by Takagi *et al.*[205]

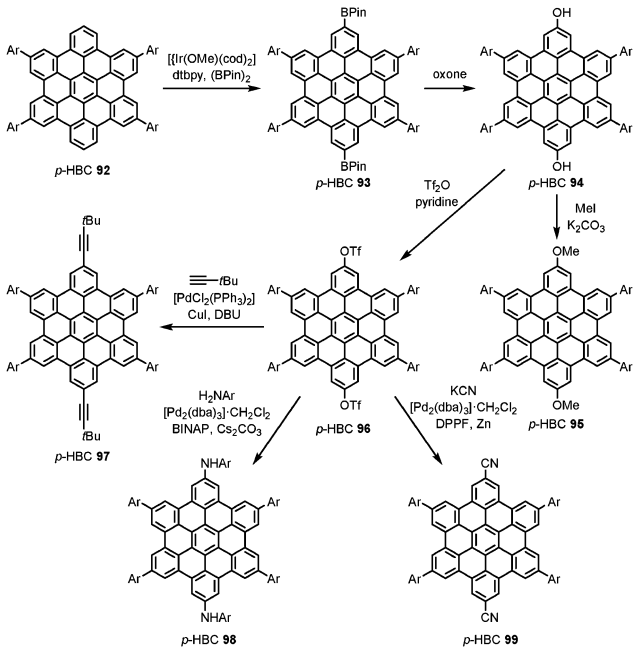

Fig. 18 Derivatizations of *p*-HBC *via* iridium-catalysed direct edge borylation. Ar: mesityl; cod: cycloocta-l,5-diene; dtbpy: 4,4′-di-*tert*-butyl-2,2′-bipyridyl; BPin: (pinacolato)boron; DBU: 1,8-diazabicyclo[5.4.0]undec-7-ene; dba: dibenzylideneacetone; BINAP: 2,2′-bis(diphenylphosphino)-1,1′-binaphthyl; DPPF: 1,1′-diphenylphosphinoferrocene.

The photophysical properties of the *p*-HBC derivatives were strongly affected by their substituents, which demonstrated the significance of such direct edge functionalization protocols to easily introduce electron-donating and electron-withdrawing groups.

The direct edge functionalization is of great importance not only for the modification of the peripheral substituents, but also for the construction of novel aromatic structures, as elegantly demonstrated by Scott, Itami *et al.* with the two-step synthesis of grossly warped graphene molecule **42** from corannulene (**39**) (Fig. 9).[127] The direct palladium-catalysed C–H arylation with *o*-chloranil as the oxidant was shown to occur exclusively at the K-regions of PAHs, which allowed their selective two-step π-extension, for instance, from phenanthrene to dibenzo[*g*,*p*]chrysene.[129] Moreover, Itami *et al.* very recently made a further advancement, realising direct one-step π-extension of PAHs at the K-regions through palladium-catalysed double C–H activation.[206] Additionally, Scott *et al.* also reported iridium-catalysed five-fold borylation of corannulene (**39**) to afford 1,3,5,7,9-pentakis(BPin)corannulene (BPin = (pinacolato)boron), which provided facile access to a defined molecular fragment of [5,5]nanotube[207] and the third synthetic route to graphene molecule **42** *via* a single isomer of precursor **40**.[127] Scott *et al.* also pioneered π-extension at the bay regions of perylene and bisanthene through the Diels–Alder reaction.[208,209] Notably, the bay regions of such PAHs can function as the dienophiles and undergo cycloadditions with activated ethylenes and acetylenes, as well as with arynes, providing facile access to PAHs extended at the bay positions.[210–213]

III. Synthesis of graphene nanoribbon

Solution-mediated synthesis of graphene nanoribbons

Whereas graphene molecules that are smaller than 5 nm can not bridge two electrodes in electronic devices, one-dimensionally extended GNRs allows fabrication of transistors based on single GNR strands, which is essential for the logic applications.[24,31] Bottom-up synthetic efforts toward GNRs date back to 1970, when Stille *et al.* reported the first attempt to synthesize a fully conjugated ladder-type polymer consisting of hexagonal and pentagonal aromatic rings.[214] Although such aromatic ladder-type polymers were not recognized as ''GNRs'' at that time, their aromatic, ribbon-like structures can indeed be viewed as GNRs with defined defects, *i.e.*, five-membered rings. Nevertheless, the ladder-type polymer obtained by Stille *et al.* was almost insoluble due to strong π–π stacking interactions, leaving the structural characterization inconclusive at that time.[215] This solubility problem was solved in 1994 by Schlüter *et al.*, who introduced flexible alkyl loops that wrapped the aromatic polymers.[215,216] Thanks to the increased solubility and improved synthetic procedure, the formation of an aromatic ladder-type polymer could be unambiguously confirmed by elemental analysis, solid-state ^{13}C NMR and transmission ultraviolet spectroscopy, as well as through investigation of structurally related model compounds.

In 1993, Scherf *et al.* reported a fully conjugated ladder-type polymer, called ''angular polyacene,'' that consisted only of six-membered rings; this polymer can be considered one of the narrowest possible GNRs with a defined structure.[217,218] The synthesis was carried out through carbonyl olefination of functionalized poly(*para*-phenylene) with B_2S_3[217,218] or through McMurry coupling.[219] In 1994, Swager *et al.* synthesized the same ladder-type polymer with different substituents through intramolecular electrophilic substitution with arylethynyl groups *via* the formation of a vinyl cations under an acidic condition.[220]

In an attempt to prepare wider ladder-type polymers, or GNRs, we have extended the nanographene synthesis based on oxidative cyclodehydrogenation to polymeric systems, using longitudinally elongated polyphenylenes as precursors.[25] Beginning in 2001, syntheses of structurally defined GNRs were attempted using A_2B_2-type Diels–Alder polymerization for the preparation of polyphenylene precursors.[221,222] However, this approach was unsuccessful because of the formation of numerous structural isomers during the polymerization step, resulting in a mixture of randomly kinked GNRs. Since 2000, Osuka *et al.* have developed the synthesis of one-dimensionally extended porphyrin tapes, achieving porphyrin 24-er in 2009 as the longest to date.[223–226] Although the porphyrin tapes are neither PAHs nor GNRs by definition, they are exquisite examples of structurally well-defined aromatic nanoribbons.

Through A_2B_2-type Suzuki polymerization. The previous synthetic attempts that employed A_2B_2-type Diels–Alder polymerization did not afford structurally defined GNRs due to the structural isomerization. Thus, we have next performed the synthesis of GNRs through A_2B_2-type Suzuki polymerization, which can circumvent this problem. In 2008, structurally well-defined and straight $N = 9$ armchair GNRs were obtained for the first time using this polymerization method.[227] With bulky alkyl chains at the peripheral positions, the GNRs were highly dispersible in organic solvents, allowing their liquid-phase processing and visualization on a graphite surface by STM. Nevertheless, the length of the observed GNRs was only up to ~12 nm, which prompted us to develop other synthetic protocols for obtaining longer GNRs, namely, by enhancing the degree of polymerization during the synthesis of the polyphenylene precursors.

The low polymerization efficiency was considered to be due to the high steric hindrance between the coupling monomers and to the high rigidity of the poly(*p*-phenylene) backbone structure. We have thus devised the use of a kinked and more flexible poly(*o*-phenylene-*p*-phenylene) **102** as a GNR precursor.[228] Polyphenylene precursor **102** was synthesized through a microwave-assisted A_2B_2-type Suzuki polymerization of *o*-dibromobenzenes **100** and benzene-1,4-diboronic ester **101** (Fig. 19). Size exclusion chromatography (SEC) analysis of the resulting polyphenylene **102b** with dodecyl chains indicated a number-average molecular weight (M_n) of 9900 g mol^{-1} and a polydispersity index (PDI) of 1.4 against a poly(styrene) (PS) standard. This M_n value corresponded to the average length of approximately 25 nm for planarized GNR **103b**, suggesting the advantage of such kinked polyphenylene backbones for the synthesis of longer GNRs *via* the A_2B_2-type Suzuki polymerization.

Noted that the ''molecular weights'' from the SEC analyses are only approximate values estimated based on available calibration curves of existing polymer standards and do not represent the absolute molecular weights, which can be measured using laser light scattering experiments.[229] Nevertheless, because the SEC molecular weights are useful for roughly comparing the sizes of polymers with similar structures, we include the SEC data in this article solely for this purpose.

In 2013, Jo and his colleagues extended the synthesis of GNR **103** by using naphthalene diboronic ester **104** and anthracene diboronic ester **107** in place of benzene diboronic ester **101** to obtain wider GNRs **106** and **109**, respectively (Fig. 19).[230] Whereas the degree of cyclodehydrogenation was demonstrated to be 100% for precursor **102** based on the relative intensities of aromatic protons in NMR spectra, the values for precursors **105** and **108** were determined to be 78% and 75%, respectively. This result suggested that cyclodehydrogenation has limited efficiency for precursors containing naphthalene or anthracene units. Notably, thin-film FET devices fabricated with GNRs **103c**, **106** and **109** all exhibited ambipolar transport properties. Wider GNRs showed higher FET performances, and GNR **109** displayed the highest hole and electron mobilities of 3.25×10^{-2} and 7.11×10^{-2} cm^2 V^{-1} s^{-1}, respectively, probably as a result of the most extended π-conjugation.

In addition to modifying the width and edge structure, heteroatom doping of aromatic frameworks is another promising method for drastically modifying the electronic properties of GNRs, as discussed above for graphene molecules. Jo *et al.* conducted N-doping of GNRs using a mixture of dibromobenzene **100** and 2,3-dibromo-5,6-bis-dodecyloxy-pyrazine in the Suzuki

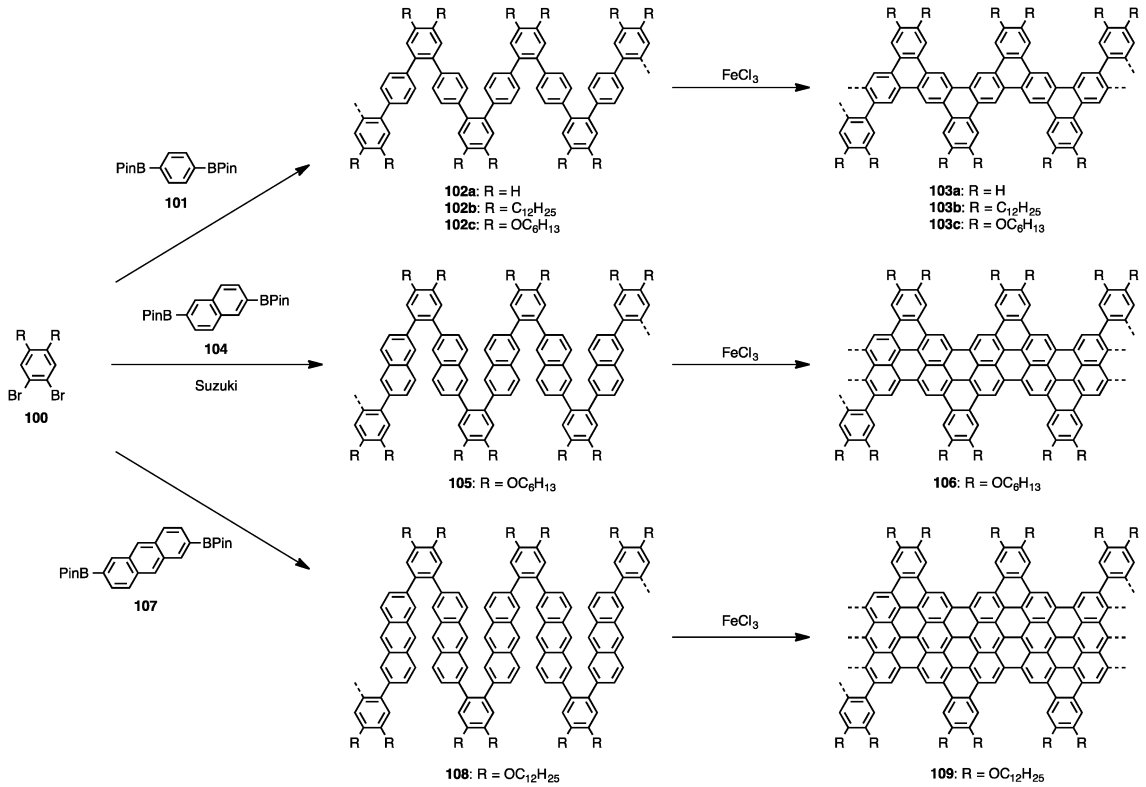

Fig. 19 Synthesis of GNRs **103**, **106** and **109** with various widths based on A_2B_2-type Suzuki polymerizations. BPin: (pinacolato)boron.

polymerization with naphthalene diboronic ester **104**.[231] By changing the mixing ratio between the dibromopyrazine and dibromobenzene **100**, GNR precursors with different degrees of N-doping could be obtained. Upon cyclodehydrogenation, 100% conversion into N-doped GNRs **110** and **111** (Fig. 20) was indicated by the NMR analysis. Notably, a higher degree of N-doping reduced the hole mobilities of the GNRs while increasing the electron mobilities. This result demonstrated that the charge-transfer behaviour of the GNRs could be tuned from ambipolar to n-type by N-doping. GNR **111** with the highest degree of N-doping exhibited the highest electron mobility of 1.02×10^{-1} cm^2 V^{-1} s^{-1}, which was two orders of magnitude higher than that of non-doped GNR **106**. Moreover, the threshold voltages of the GNRs varied from +20 V for non-doped GNR **106** to −6 V for N-doped GNR **111**.

We have also synthesized GNR **114** featuring a unique "necklace-like" structure through the A_2B_2-type Suzuki polymerization of

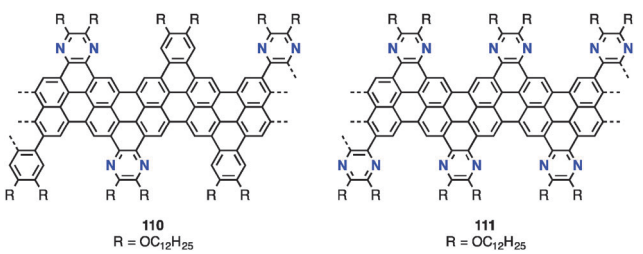

Fig. 20 Structures of N-doped GNRs **110** and **111** prepared through A_2B_2-type Suzuki polymerizations.

4,4′-dibromobiphenyl-based precursor **112** and benzene-1,4-diboronic ester **101** (Fig. 21).[232] Polyphenylene precursor **113** was obtained with a weight-average molecular weight (M_w) of 6900 g mol^{-1} and a PDI of 1.7 according to SEC analysis against a PS standard. MALDI-TOF MS analysis of precursor **113** displayed mass peaks up to m/z = 17 000, corresponding to **113** with ten repeating units, which converted to GNR **114** with the length of approximately 13 nm. The UV-Vis absorption spectrum of GNR **114** revealed its relatively smaller optical bandgap of ~1.4 eV, which was in line with the DFT calculation.

Through AA-type Yamamoto polymerization. Although the use of the A_2B_2-type Suzuki polymerization enabled the preparation of various structurally defined GNRs, the longitudinal extensions of these GNRs, *i.e.*, molecular weights of the polyphenylene precursors, were limited. This restriction was possibly a result of the inefficiency of the A_2B_2-type Suzuki polymerization and/or the necessity of two different monomers causing stoichiometry problems.[233,234] The heterogeneous biphasic conditions of the Suzuki polymerization might also have a detrimental effect. Therefore, AA-type Yamamoto polymerization was considered to be more advantageous because this method requires only one dihalogenated monomer and is thus free of the stoichiometry problem. Moreover, the Yamamoto coupling is also known to be highly efficient in sterically hindered systems,[235,236] which is important for the preparation of sterically congested GNR precursors.

In 2012, we synthesized laterally extended GNR **117** through the AA-type Yamamoto polymerization of dichlorinated monomer **115** (Fig. 21).[237] Notably, the Yamamoto polymerization of

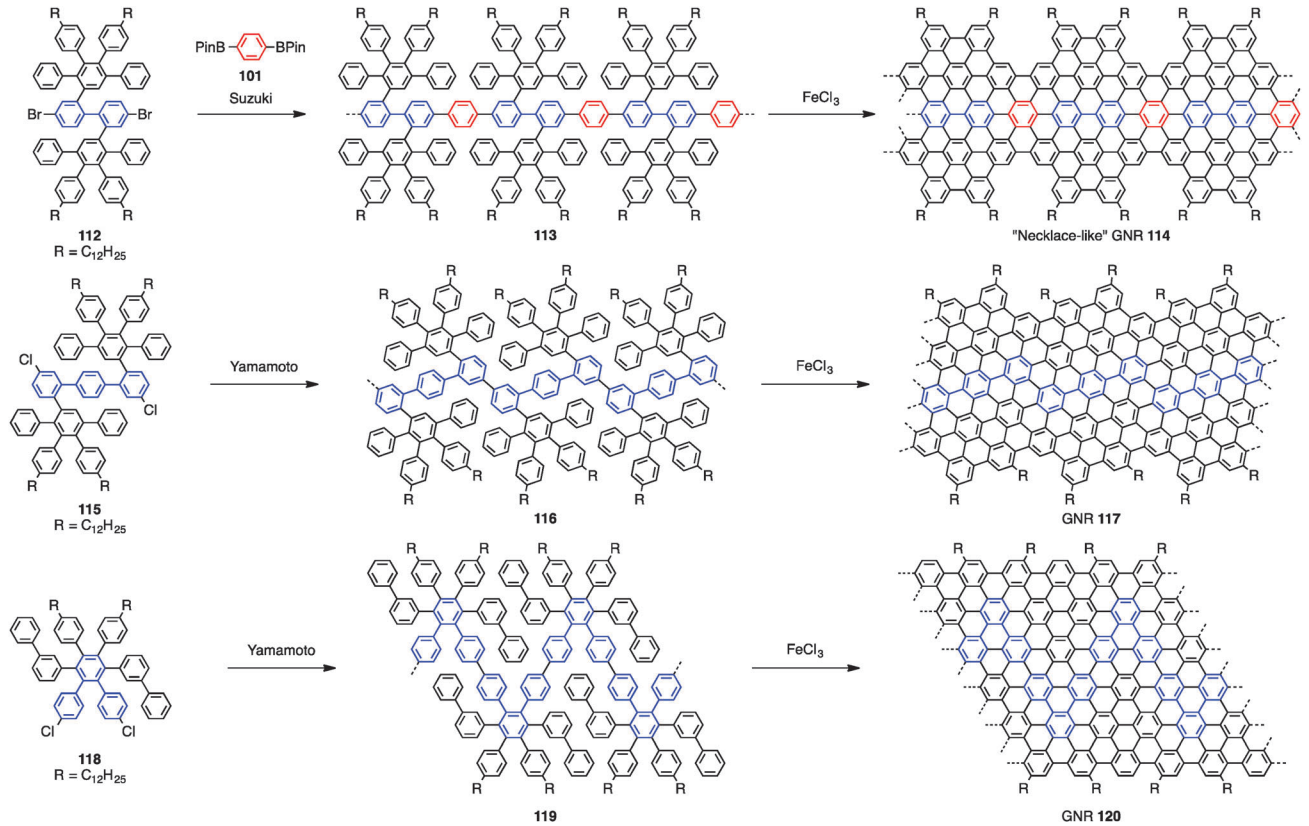

Fig. 21 Synthesis of "necklace-like" GNR **114** through A_2B_2-type Suzuki polymerization of naphthalene-based monomer **112** and laterally extended GNRs **117** and **120** through AA-type Yamamoto polymerizations of *p*-terphenyl-based monomer **115** and *o*-terphenyl-based monomer **118**, respectively. Obtained GNR **120** was rather short and mixed with shorter graphene molecules.

115 proceeded very efficiently, yielding polyphenylene precursor **116** with an M_w of 52 000 g mol^{-1}, an M_n of 44 000 g mol^{-1} and a PDI of 1.2 according to SEC analysis against a PS standard, which were clearly higher than the molecular weights achieved using the A_2B_2-type Suzuki polymerization. The laterally extended GNR **117** with an estimated width of 1.54–1.98 nm featured a significantly lowered optical bandgap of approximately 1.1 eV with broad absorption into the near-infrared region of the optical spectrum.

We have next attempted a synthesis of even wider GNR **120** with an estimated width of ~2.1 nm, corresponding to $N = 18$ armchair GNR, by employing monomer **118** (Fig. 21).[238] While monomer **115** with a dichlorinated *p*-terphenyl backbone structure yielded GNR **117** with the same width as **115**, monomer **118** with a dichlorinated *o*-terphenyl backbone led to GNR **120**, which was twice as wide as the monomer. However, the AA-type Yamamoto polymerization of monomer **118** afforded polyphenylene precursor **119** with a relatively low M_w of 10 000 g mol^{-1}, an M_n of 7200 g mol^{-1} and a PDI of 1.4 based on SEC analysis against a PS standard, presumably because of high steric hindrance during the polymerization. The observed optical bandgap of GNR **120** was approximately 1.6 eV. These results indicated that the obtained GNR **120** was rather short, and mixed with oblong-shaped graphene molecules, based on the definition given in the introduction. Additionally, such relatively large graphene molecules could be successfully sublimed and integrated into FET devices through vapour-phase transport deposition, showing better on–off ratio compared to those processed from a liquid phase.[239]

In 2014, Sinitskii *et al.* reported the gram-scale synthesis and comprehensive characterizations of chevron-type GNR **123** through the AA-type Yamamoto polymerization of 6,11-dibromo-1,2,3,4-tetraphenyltriphenylene (**121**)[240] and subsequent cyclodehydrogenation (Fig. 22).[241] GNR **123** had previously been prepared in our group using the solution synthesis[242] as well as the surface-assisted method[37] as will be discussed in the next section. Nevertheless, they have demonstrated the well defined structure of the solution synthesized GNR **123** for the first time using STM under UHV conditions, clearly observing the planarization of three-dimensional precursor **122** into planar GNR **123**.[241] UV-Vis absorption measurements of GNR **123** in a dispersion revealed its optical bandgap of approximately 1.6 eV.[243]

Moreover, using the same synthetic strategy, Sinitskii *et al.* conducted a solution synthesis of N-doped, chevron-type GNR **126**, starting from 5-(6,11-dibromo-1,3,4-triphenyltriphenylen-2-yl)pyrimidine (**124**) (Fig. 22).[244] STM analysis revealed a defined structure of GNR **126** similar to that of GNR **123**, and energy-dispersive X-ray (EDX) and X-ray photoelectron spectroscopy (XPS) measurements corroborated the successful N-doping. The optical

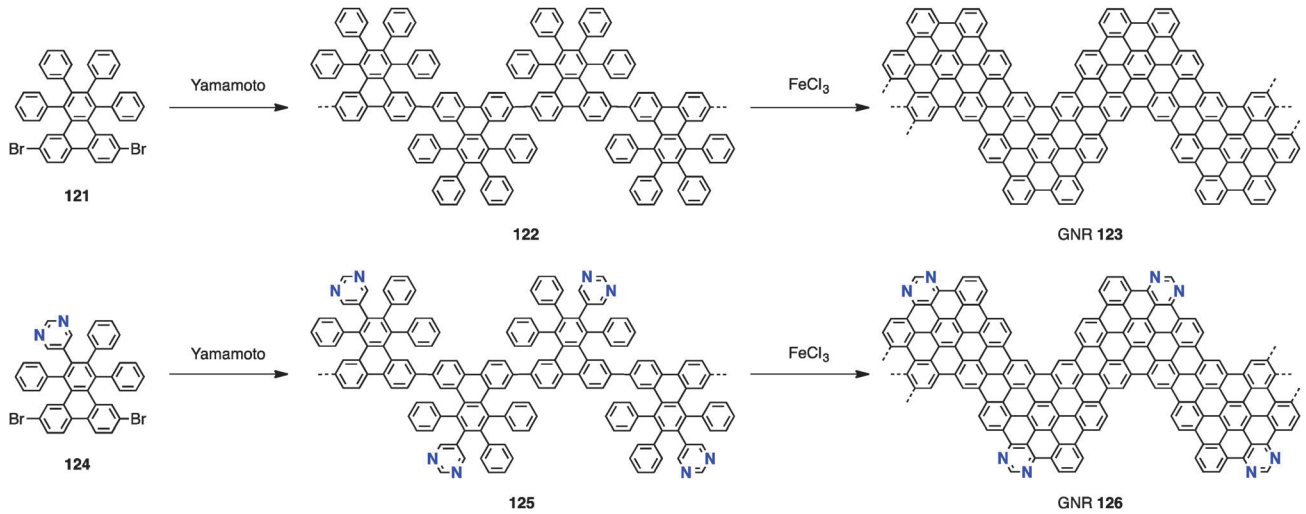

Fig. 22 Synthesis of pristine and N-doped chevron-type GNRs **123** and **126**, respectively, based on AA-type Yamamoto polymerizations. N-doped precursor **125** and GNR **126** are obtained as mixtures of structural isomers.

bandgap of GNR **126** was derived from its UV-Vis absorption spectrum to be approximately 1.6 eV, which was the same as that in its non-doped analogue, GNR **123**.

Through AB-type Diels–Alder polymerization. The use of the AA-type Yamamoto and A_2B_2-type Suzuki polymerization methods has enabled bottom-up synthesis of structurally defined GNRs with different widths and edge structures, reaching a length of >100 nm with chevron-type GNR **123**.[241]

However, such metal-catalysed coupling reactions are generally limited by the use of expensive catalysts and relatively low molecular weights, in most cases leading to GNRs shorter than 50 nm. Turning back to the traditional polyphenylene synthesis, the Diels–Alder reaction is still appealing because it reproducibly offers M_w values higher than 100 000 g mol^{-1} based on SEC analyses in many systems.[221,245,246] Moreover, no catalyst or additive is necessary for the Diels–Alder reaction, which is highly advantageous for larger-scale syntheses.

In 2014, we have for the first time reported an AB-type Diels–Alder polymerization to prepare GNR **129** with a "cove-type" edge structure, which simultaneously enabled unprecedentedly high longitudinal extension over 600 nm (Fig. 23).[229] King *et al.* has coined a term "gulf" for such edge configuration in 2008,[199] but we use the term "cove-type" for these GNRs in this review, following older literature.[9,40,81] In this approach, tetraphenylcyclopentadienone-based monomer **127** was rationally designed such that all the structural isomers of the resulting precursor **128**

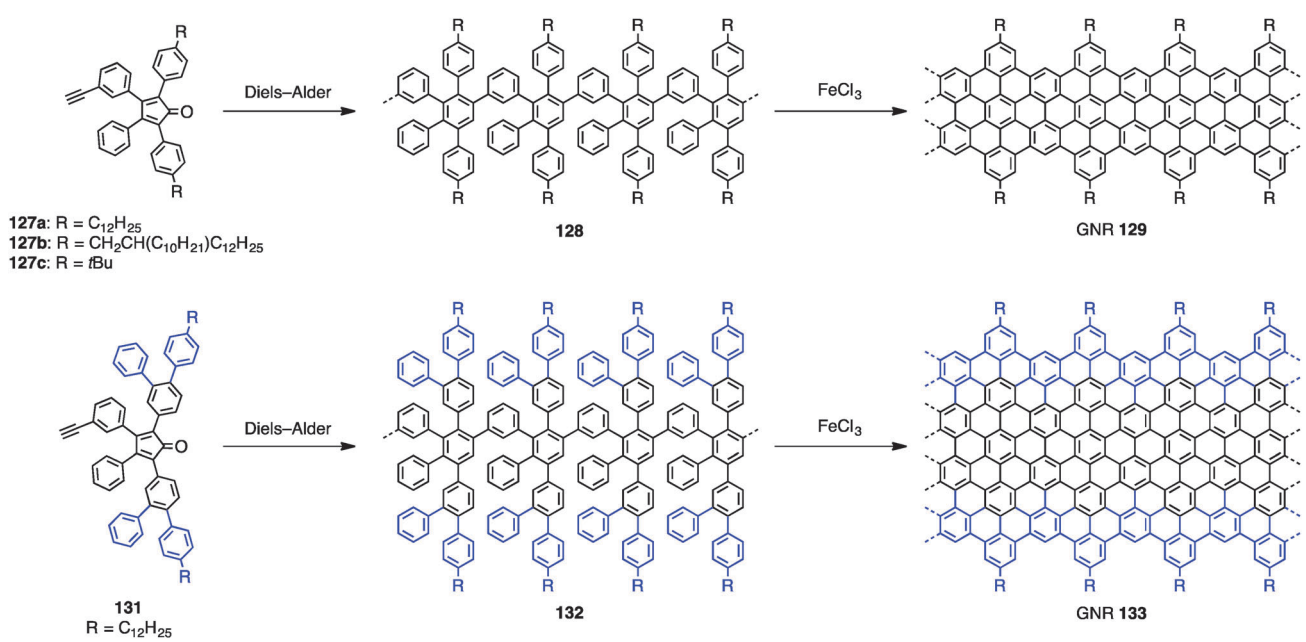

Fig. 23 Synthesis of GNRs **129** and **133** through AB-type Diels–Alder polymerization of monomers **127** and **131**, respectively.

would lead to a single, straight GNR **129** with an estimated width of 0.69–1.13 nm (Fig. 23).[229] Furthermore, C–C bond formation at undesired positions during the cyclodehydrogenation of **128** is hindered by the steric repulsion between benzene rings and bulky alkyl chains, ensuring the non-kinked and uniform structure of the resulting GNR **129**.

The AB-type Diels–Alder polymerization of monomer **127a** afforded precursor **128a** with a markedly high M_w of 640 000 g mol^{-1}, an M_n of 340 000 g mol^{-1} and a PDI of 1.9 based on SEC analysis, thereby proving the remarkably high efficiency of this polymerization method. The UV-Vis absorption spectrum of GNR **129** revealed a large optical bandgap of ~1.9 eV, which was in excellent agreement with theoretical predictions.[247] The edge chlorination method developed for the graphene molecules (Fig. 16) also proved to be applicable for GNR **129c** to afford chlorinated GNR **130**, which demonstrated lowered optical bandgap as expected by the theory (Fig. 24).[198,247]

Furthermore, deposition of isolated strands of GNR **129a** was achieved by immersing a functionalized Si/SiO_2 substrate in a diluted dispersion of **129a**, demonstrating that the GNRs extended over 600 nm.[249,250] By treating the Si/SiO_2 substrate with silane derivatives with different hydrophobicities, it is possible to control the density of the deposited GNRs.[250] Transistor devices could be fabricated by directly depositing metal electrodes on such GNR strands, which exhibited good electrical conduction through the isolated GNRs.[249,251]

In 2014, we have achieved lateral extension of GNR **129** by using monomer **131** with four additional benzene rings at the peripheries of monomer **127** (Fig. 23).[252] Notably, the Diels–Alder polymerization of monomer **131** led to polyphenylene precursor **132** with a high M_w of 550 000 g mol^{-1}, an M_n of 150 000 g mol^{-1} and a PDI of 3.8 based on SEC analysis against the PS standard, which was comparable to the highest molecular weight values obtained for the narrower precursor **128**. The resulting GNR **132** exhibited broad absorption profile into the NIR region with a lowered optical bandgap of approximately 1.2 eV, which was in good agreement with the DFT-calculated bandgap.[253] Ultrafast terahertz (THz) photoconductivity measurements demonstrated excellent intrinsic mobility of GNR **132**, similar to that of the narrower GNR **129a**.[248] Moreover, the broad absorption of GNR **132** enabled spectroscopic characterizations at a wider range of wavelengths, as represented by Raman and pump–probe THz photoconductivity analyses, which is indispensable for in-depth studies on the fundamental properties of such GNR structures.

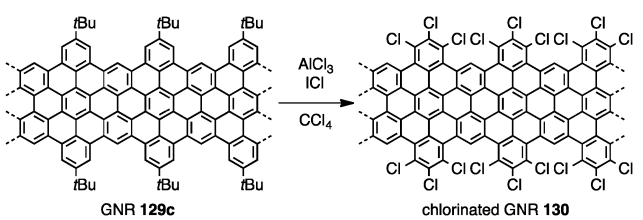

Fig. 24 Edge chlorination of GNR **129c** to GNR **130**.

Surface-assisted synthesis of graphene nanoribbons

Synthesis under UHV conditions. A number of structurally defined GNRs with different widths, edge structures and heteroatom doping have been successfully synthesized based on the solution-mediated method, as discussed in the previous section. However, microscopic visualization with atomic resolution and in-depth physical characterizations of such GNRs have remained a challenge because of their strong aggregation tendency and the difficulty of placing isolated strands of such GNRs on a surface without any contamination. In 2010, in collaboration with Fasel and his colleagues, we have developed a complementary approach to this solution synthesis, *i.e.*, direct growth of GNRs on metal surfaces under UHV conditions.[37] Using this surface-assisted method, atomically precise structures of the resulting GNRs can be clearly observed *in situ* using the state-of-the-art high-resolution STM.

This method combines the surface-assisted coupling of aryl halides developed for the preparation of molecular wires[254] and covalently bonded networks[255–257] with surface-catalysed cyclodehydrogenation, which we demonstrated for the synthesis of a defined triangular PAH, tribenzo[*a*,*g*,*m*]coronene, from a cyclic polyphenylene, cyclohexa-*o*-*p*-*o*-*p*-*o*-*p*-phenylene.[258] In the surface synthesis of the GNRs, the corresponding polyphenylene precursors are first fabricated from rationally designed, dihalogenated monomers through the surface-assisted coupling of aryl halides. Here, biradical intermediates are generated through carbon–halogen bond cleavage upon thermal treatment of the monomer on the surface, followed by radical polymerization. Subsequently, the polyphenylene precursors are ''planarized'' and ''graphitized'' through surface-catalysed cyclodehydrogenation by annealing at higher temperatures to produce the desired GNRs. All these processes can be monitored using high-resolution STM, allowing full control over each synthetic step.

With Fasel and his colleagues, we have performed the first attempt for the surface-assisted synthesis of GNRs using 6,11-dibromo-1,2,3,4-tetraphenyltriphenylene (**121**) as the starting monomer,[37] which we had previously synthesized as the monomer of blue-light-emitting polymer **122**[240] as well as for the solution synthesis of chevron-type GNR **123**[259] (Fig. 22). Remarkably, monomer **121** could be polymerized to polyphenylene **122** upon sublimation onto a Au(111) surface and thermal activation at 250 °C, followed by planarization and graphitization at 440 °C into atomically precise GNR **123** with the length of up to approximately 100 nm,[260] which could be revealed by *in situ* high-resolution STM analysis.

By using 10,10′-dibromo-9,9′-bianthryl (**134**) as the monomer instead of monomer **121**, we could obtain $N = 7$ armchair GNR **136** in a similar manner (Fig. 25a), which could clearly be visualized by *in situ* high-resolution STM (Fig. 25b).[37] STS measurements revealed that the electronic bandgap of GNR **136** is 2.3 eV on the Au(111) surfaces[261] in agreement with the theoretical estimation.[262] Following our report, many other research groups have successfully prepared and studied atomically precise GNR **136**. Grill *et al.* measured the conductivity of a single nanoribbon of **136** using an STM pulling technique.[263]

Liljeroth and Swart *et al.* obtained atomically resolved AFM images of GNR **136** and demonstrated creation of a single GNR-Au bond by removing one hydrogen atom with a local high voltage pulse.[264] Moreover, Huang and Wee *et al.* showed that $N = 7$ GNR **136** could be fused in parallel with neighbouring nanoribbons on Ag(111) surfaces, leading to the formation of $N = 14$ and 21 armchair GNRs.[265]

Spatially aligned GNRs can be grown by using stepped Au(788) surfaces, in contrast to the formation of randomly oriented GNRs on Au(111) surfaces. This spatial alignment allowed the detailed investigation of the occupied electronic states of the GNRs through angle-resolved UV photoemission spectroscopy (ARUPS).[260,261] Such spatially well-aligned GNRs also enabled studies of their optical properties on the metal surfaces using reflectance difference spectroscopy (RDS), revealing the strong anisotropy of GNR **136** and its optical bandgap of 2.1 eV.[262] The difference between this optical bandgap and the DFT-calculated electronic bandgap of 3.7 eV could be explained by the exciton binding energy. On the other hand, the electronic bandgap observed by the STS analyses was revealed to be reduced by the polarization of the metallic substrates.[262]

In 2014, Han and Asao *et al.* demonstrated that the same monomer **134** undergoes intermolecular cyclodehydrogenation at different configurations on a Cu(111) surface, leading to an unprecedented formation of chiral-edge (3,1)-GNR **137** with atomic precision (Fig. 25a and c).[266] In contrast to the GNR synthesis on a Au(111) surface, where the biradical intermediates can freely diffuse, the monomers on a Cu(111) surface are demobilized even at elevated temperatures and the cyclodehydrogenation occurs only inside preassembled domains. Thus the resulting GNRs are distributed along distinct directions relative to the Cu(111) atomic rows, which is predetermined by the self-assembly of the monomers.

By extending dibromobianthryl monomer **134** to 2,2′-di[(1,1′-biphenyl)-2-yl]-10,10′-dibromo-9,9′-bianthracene (**138**) with two extra biphenyl units at the peripheries, Fischer, Crommie, and co-workers achieved a selective synthesis of laterally extended $N = 13$ armchair GNR **140** on a Au(111) surface and visualized

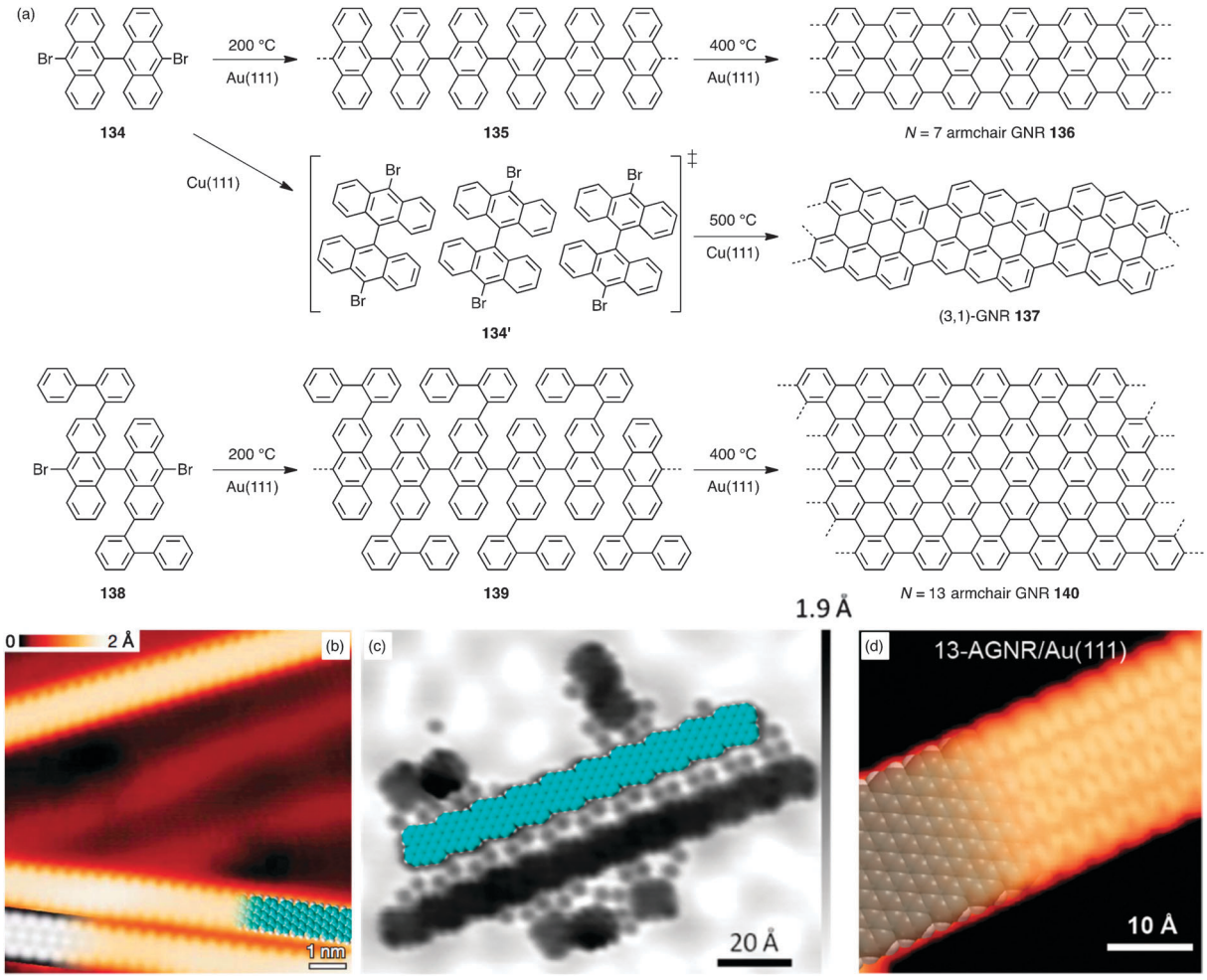

Fig. 25 (a) Surface-assisted synthesis of $N = 7$ armchair GNR **136**, chiral (3,1)-GNR **137**, and $N = 13$ armchair GNR **140**. (b)–(d) STM images of (b) GNR **136** on an Au(111) surface, (c) GNR **137** on a Cu(111) surface, and (d) GNR **140** on an Au(111) surface with (b and d) partly or (c) completely overlaid molecular models (light blue). Panel b also shows partially overlaid DFT-based STM simulation (gray scale). The circular features in panel c are bromine atoms trapped between GNRs. (b) Reprinted by permission from Macmillan Publishers Ltd: *Nature* (ref. 37), Copyright (2010). (c) and (d) Reprinted with permission from (c) ref. 266; Copyright 2014 and (d) ref. 267; Copyright 2013, American Chemical Society.

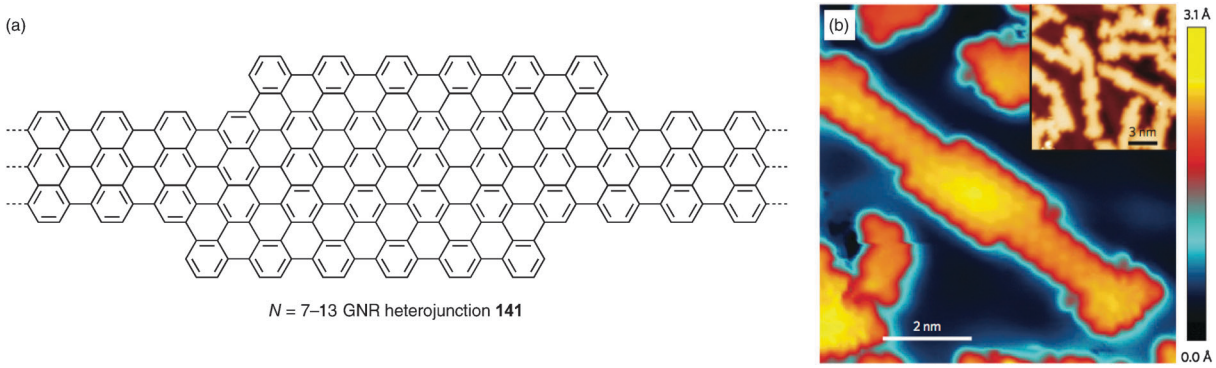

Fig. 26 (a) Chemical structure of N = 7–13 GNR heterojunction **141** and (b) its high-resolution STM image on an Au(111) surface. Inset: STM image of a larger area, showing various N = 7–13 GNR heterojunctions. Reprinted by permission from Macmillan Publishers Ltd: *Nature Nanotechnology* (ref. 39), Copyright (2015).

its atomically precise structure by high-resolution STM (Fig. 25a and d).[267] STS analysis revealed the electronic bandgap of N = 13 GNR **140** on Au(111) to be approximately 1.4 eV, which was approximately 1 eV smaller than the STS bandgap of N = 7 GNR **136**.[261,263]

In 2015, these authors reported a GNR heterojunction or block copolymer, consisting of two GNR segments with different widths.[39] Through co-sublimation of monomers **134** and **138**, a mixture of N = 7–13 GNR heterojunctions such as **141** could be obtained, as revealed by *in situ* STM observation (Fig. 26). STM and STS investigations revealed that the N = 7–13 GNR heterojunctions have height-dependent electronic structures, which are similar to that of type I semiconductor junctions, thereby demonstrating molecular bandgap engineering in a single strand of GNR.

In the same year, with Fuchs and Chi we described a surface synthesis of N = 5 armchair GNRs on Au(111), starting from 1,4,5,8-tetrabromonaphthalene (**142**) as the monomer (Fig. 27a and b).[268] In contrast to above-mentioned examples, the preparation of GNR **142** did not require the final cyclodehydrogenation step and could be completed at significantly lower temperature, *i.e.*, ~300 °C. High-resolution STM analyses demonstrated that Au–naphthalene hybrid, bis(1,8-naphthylene)diaurate, was formed as an intermediate, which enabled the selective synthesis of the desired N = 5 armchair GNR structure.

Moreover, with Ruffieux and Fasel we developed a synthetic route toward cove-edged GNR **146** employing 11,11′-dibromo-5,5′-bischrysene (**144**) as the monomer (Fig. 27a and c).[108] Whereas a variety of GNRs with armchair-type edges have been achieved, GNR **146** is the first GNR with the cove edge structure. Short dimer and tetramer of GNR **146** were separately synthesized in solution as model compounds, and single-crystal X-ray analysis of the tetramer revealed non-planar structures of such cove-edged GNRs with alternate "up-down" conformations of the peripheral benzene rings. DFT calculations predicted a bandgap of 1.70 eV for cove-edged GNR **146**, which is relatively lower than that of slightly broader GNR **129**.[253]

Whereas most of the surface fabrication of GNRs has thus far been performed with triphenylene- and bianthryl-based monomers **121** and **134**, respectively, and their derivatives, it

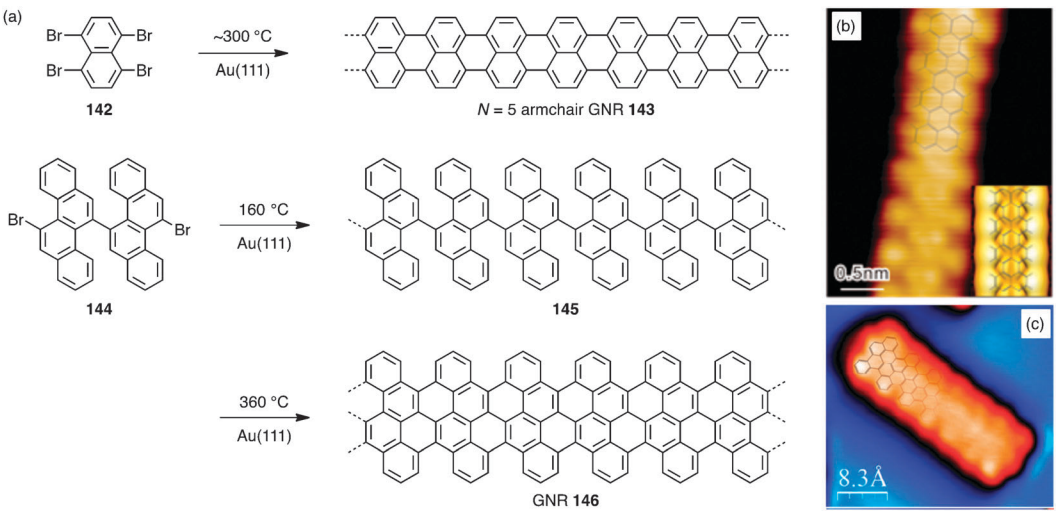

Fig. 27 (a) Surface-assisted synthesis of N = 5 armchair GNR **143** and cove-edged GNR **146**. (b and c) STM images on Au(111) surfaces of (b) GNR **143** and (c) GNR **146**.[108] (b) Inset: DFT-simulated STM image of GNR **143**. Reprinted with permission from ref. 268; Copyright 2015, American Chemical Society.

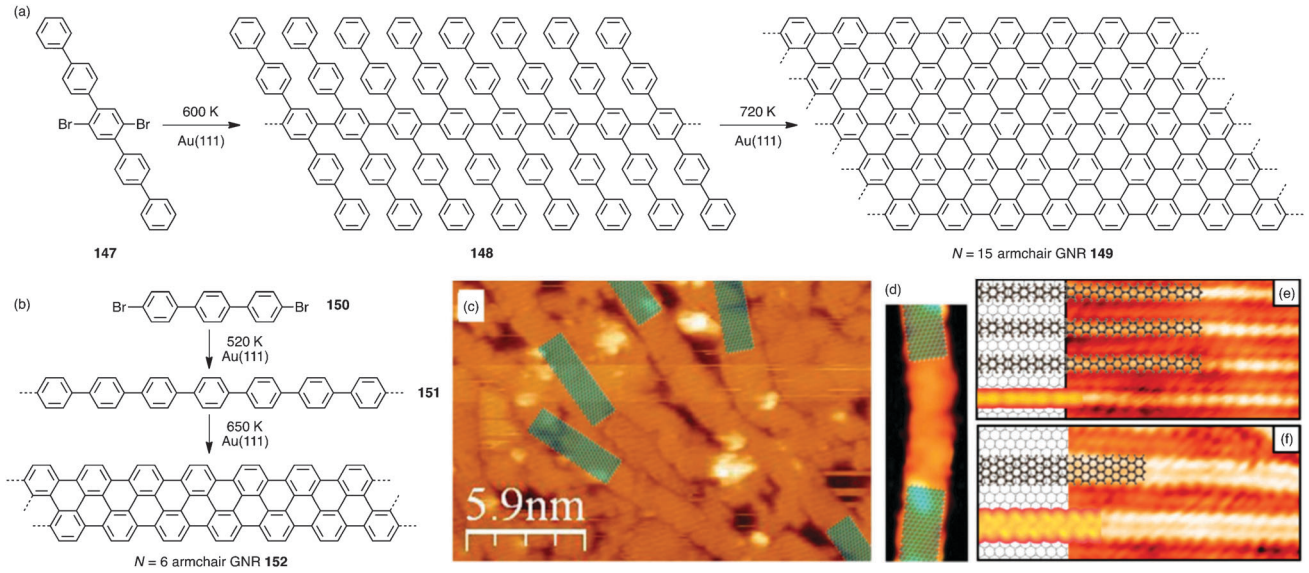

Fig. 28 Surface-assisted syntheses of (a) N = 15 armchair GNR **149** from dibromo-*p*-pentaphenyl **147** and (b) N = 6 armchair GNR **152** from dibromo-*p*-terphenyl **150**. (c)–(f) STM images of (c), (d) GNR **149**, (e) PPP **151** and (f) GNR **152** on Au(111) surfaces with partly overlaid molecular models. (c and d) Reprinted from ref. 269, Copyright (2014), with permission from Elsevier. (e and f) Reprinted with permission from ref. 270; Copyright 2015, American Chemical Society.

is also possible to design feasible syntheses based on simpler oligophenylene monomers. In 2014, Amsharov *et al.* reported an attempt to synthesize N = 15 armchair GNR **149** from dibromo-*p*-pentaphenyl **147** as the monomer (Fig. 28a).[269] STM analysis revealed the formation of broad GNRs with a width of 2.1 nm, consistent with the molecular models (Fig. 28c and d). However, a certain amount of defects could not be avoided, suggesting difficulties in fabricating atomically precise N = 15 GNR **149** from this monomer. In 2015, Basagni and Sedona *et al.* reported the synthesis of N = 6 armchair GNR **152** from dibromo-*p*-terphenyl **150** through the formation of poly(*para*-phenylene) (PPP **151**) and subsequent fusion of neighbouring PPPs (Fig. 28a).[270] By controlling the annealing temperature, PPP **151** and GNR **152** could be obtained with high selectivity and their atomically precise structures were revealed by STM observations (Fig. 28e and f, respectively). Additionally, Endo *et al.* showed that GNRs can be prepared on a Au(111) surface from *n*-alkane as the monomer, but precise structural control remains elusive.[271]

N-doping of GNRs under UHV conditions. Similar to the solution-mediated synthesis, selectively N-doped GNRs can be fabricated on metal surfaces under UHV conditions by using N-doped monomers.[38,272,273] For example, Bronner, Hecht and Tegeder *et al.* reported that the use of 4,4′-(6,11-dibromo-1,4-diphenyltriphenylene-2,3-diyl)dipyridine (**153**) as the monomer led to the formation of N-doped GNR **155** on a Au(111) surface, following the procedure developed for the preparation of non-doped GNRs (Fig. 29a).[272] With Du and Gao we revealed atomically precise structures of N-doped GNR **155** by high-resolution STM, showing an interesting side-by-side alignment with the neighbouring GNRs in an antiparallel arrangement, which was slightly shifted to maximize the attractive N···H interactions (Fig. 29b).[273] Such alignment was not observed for non-doped chevron-type GNR **123**, which showed apparently no interaction between two GNRs.[37,38]

Moreover, chevron-type GNRs with different degree of N-doping could be synthesized, containing one, two or four nitrogen atoms in each repeating unit, by employing tetraphenyltriphenylene-based monomers with different degrees of N-doping, such as **153** and 5,5′-(6,11-dibromo-1,4-diphenyltriphenylene-2,3-diyl)dipyrimidine (**156**) (Fig. 29).[38,272,273] Theoretical as well as experimental investigations showed that the N-doping drastically lowered the electronic energy levels of the GNRs to induce n-type semiconductor properties, while not significantly affecting the bandgap. The shift of the energy levels critically depends on the degree of N-doping, which enabled precise tuning of the energy offset by molecularly controlling the degree of the doping.

In 2014, together with Fasel and co-workers, we reported the synthesis of GNR heterojunction **157**, consisting of short segments of N-doped and non-doped chevron-type GNRs, through the alternating deposition of N- and non-doped monomers **156** and **121**, respectively (Fig. 29a).[38] In an STM image of GNR heterojunction **157**, the N-doped GNR segment cannot be distinguished from the non-doped segment at first glance, but the attractive antiparallel alignment between the N-doped segments provides an indication (Fig. 29c). Moreover, the differential conductance dI/dV maps exhibited a clear inversion of the contrast when measured at bias voltages of −0.35 and −1.65 V (Fig. 29e and f, respectively), which enabled assignment of the N-doped and non-doped segments as highlighted in blue and light grey, respectively, in Fig. 29d. GNR heterojunction **157** featured a type II staggered gap configuration with a band offset of ~0.5 eV, thus realizing a molecular p–n junction in a single GNR.

Although the surface-assisted synthesis enabled the preparation and characterization of atomically precise GNRs with

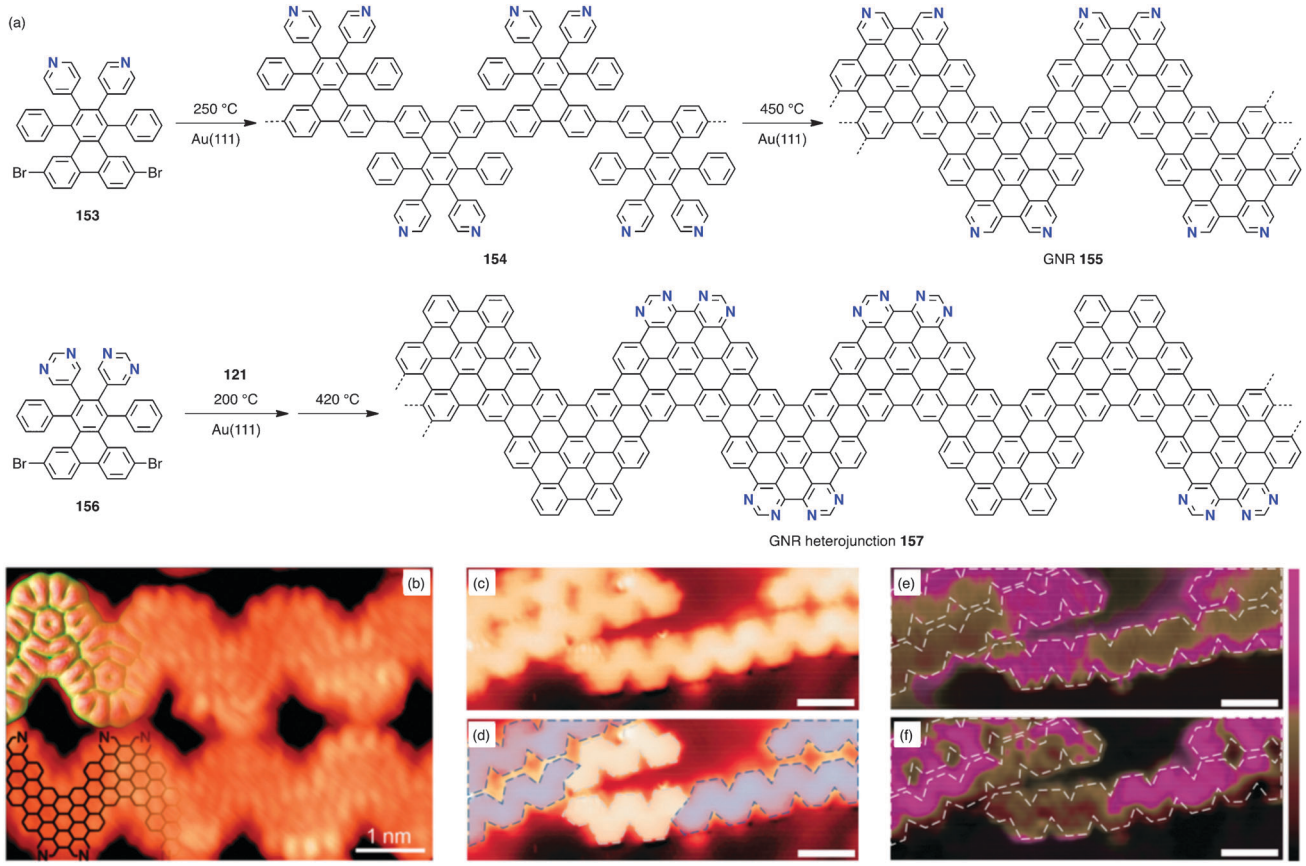

Fig. 29 (a) Surface-assisted synthesis of N-doped chevron-type GNR **155** and GNR heterojunction **157**. (b) High-resolution STM image of N-doped GNR **155**, showing an antiparallel alignment to maximize the attractive N···H interactions. DFT-based STM simulation model and a formula chemical structure are partially overlaid. Reprinted with permission from ref. 273; Copyright 2014, AIP Publishing LLC. (c and d) STM images of GNR heterojunction **157**. In panel d, the N-doped and non-doped GNR segments are highlighted in blue and light grey, respectively, as determined from the panels e and f. (e and f) Differential conductance d*I*/d*V* maps observed at bias voltages of (e) −0.35 V and (f) −1.65 V. The heterostructure profiles seen in the panel c are drawn as blue or white dashed lines in panels d–f as a guide to the eye. Scale bars in panels (c)–(f) indicates 2 nm. Adapted by permission from Macmillan Publishers Ltd: *Nature Nanotechnology* (ref. 38), Copyright (2014).

different widths, edge structures, heteroatom doping and heterojunctions, such GNRs are all bound to the metal surfaces and thus cannot be directly integrated into electronic devices. This makes it imperative to develop a reliable method for cleanly transferring the GNRs from the metal surfaces onto Si/SiO_2 or other dielectric substrates. One way to achieve this is to grow the GNRs on epitaxial Au(111) films on mica substrates. Both the mica substrates and the thin gold films can be easily removed from the GNRs, allowing their transfer onto an arbitrary substrate, such as SiO_2, CaF_2, and Al_2O_3.[38] This transfer method allowed the fabrication of working FET devices based on surface-synthesized GNRs.[274] Nevertheless, further improvements in the transfer and device fabrication processes are needed to obtain GNR-based FET devices with the high performance predicted by theoretical studies. On the other hand, the direct growth of GNRs on insulating substrates is more desirable because it will allow for the fabrication of electronic devices without the complicated transfer process. One possible way to achieve this goal is to use photo-induced coupling of dibrominated monomers followed by graphitization under e-bean irradiation.[275] Using this method, monomer **134** could indeed be converted to GNR-like structures on a mica substrate, although obtaining precise structural control is still in progress.

Synthesis under CVD conditions. The surface-assisted GNR synthesis can reliably produce atomically precise structures, but this method under UHV conditions requires complex and expensive setups and is highly time-consuming, which hinders the preparation of large amounts of GNRs and thus their practical application. Therefore, it is straightforward to attempt to synthesize GNRs under low-vacuum conditions with simpler setups. In 2014, Sakaguchi and Nakae *et al.* reported the fabrication of GNR films under CVD conditions at a pressure of 1 Torr with a flow of argon gas.[276] The synthesis was performed by annealing dihalogenated monomers on Au(111) surfaces, similar to the UHV method. Monomer **134**, a mixture of 3,9-dibromoperylene and 3,10-dibromoperylene, and 1,4-bis(4-bromophenyl)-2,3,6,11-tetraphenyltriphenylene were employed as monomers to obtain bulk films of multilayer GNRs with three different widths, corresponding to $N = 7$, 5 and 9 armchair GNRs, respectively.

The GNR films CVD-grown on Au(111) surfaces could be transferred onto any substrate using a wet process, which

enabled UV-Vis absorption analysis of the GNRs. The absorption spectra revealed optical bandgaps of 0.8, 1.6 and 1.3 eV for N = 5, 7 and 9 GNRs, respectively, which was in agreement with the theoretically predicted trend. FET devices were also fabricated on transferred GNR films, exhibiting a charge-carrier mobility of up to 10^{-4} cm^2 V^{-1} s^{-1}. Moreover, the GNR films also showed photoconductivity with a current gain upon illumination of up to 7.3%, which is better than the value of 2.7% measured for P3HT. This result indicated that such CVD-grown GNRs could function as excellent photoconductors. Nevertheless, more detailed studies and comprehensive characterizations are necessary to elucidate if the CVD-grown GNRs are chemically identical as GNRs fabricated from the same monomers under the UHV conditions.

Synthesis of GNRs confined in carbon nanotubes

Bottom-up GNR synthesis has also been reported through thermal or electron (e)-beam mediated polymerization and fusion of aromatic molecules that are confined inside single-walled CNTs (SWCNTs).[277–279] In 2011, Talyzin and Anoshkin *et al.* demonstrated that perylene and coronene confined in SWCNTs could be converted into GNRs encapsulated in the SWCNTs (GNR@SWCNT) by heating at approximately 400–500 °C (Fig. 30a).[277] The aromatic molecules were closely aligned one-dimensionally inside the SWCNT, enabling the polymerization and fusion into GNRs. The structures of the resulting GNRs were dependent on the starting monomer. In 2015, Shinohara *et al.* succeeded in studying the optical properties of the GNRs inside SWCNTs by covalent functionalization of the nanotube walls with 4-bromobenzenediazonium tetrafluoroborate.[280] The excitonic absorption peaks of the nanotubes were efficiently suppressed, revealing the optical transitions of the coronene-based GNRs at 1.5 and 3.4 eV.

In 2011, Khlobystov *et al.* reported the fabrication of GNR@SWCNT with sulphur-terminated edges from S-containing fullerene derivative **158** (Fig. 30b) or a mixture of pristine fullerene and tetrathiafulvalene (TTF) confined in SWCNTs.[278] By e-beam irradiation, such monomers could be fused to S-doped GNRs inside a SWCNT, where the S atoms terminated the reactive edges of the as-formed GNRs (Fig. 30c–e). This is in contrast to the fact that pristine fullerenes are transformed into narrower guest-SWCNTs inside host-SWCNTs through a similar treatment.[281] Additionally, such S-doped GNRs could also be generated from TTF alone confined in SWCNTs.[278,279] The GNRs fabricated inside the SWCNTs feature highly uniform widths and very smooth edge structures compared to top-down fabricated GNRs, but the structural precision achievable by this method is considerably lower than that of the other bottom-up synthetic approaches described in the previous section. Moreover, selective removal of the CNTs without affecting the confined GNRs is highly challenging, hindering further studies and application of such GNRs.

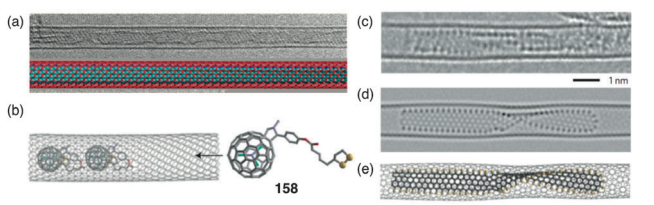

Fig. 30 (a) A TEM image of a GNR@SWCNT prepared from coronene (top) and its model (bottom); light blue: GNR, red: SWCNT. Reprinted with permission from ref. 277; Copyright 2011, American Chemical Society. (b) A schematic illustration of the confinement of fullerene derivative **158** in a SWCNT; grey: carbon, red: oxygen, purple: nitrogen, yellow: sulphur. (c) An aberration-corrected high-resolution TEM image, (d) a simulated TEM image, and (e) a molecular model of a GNR with sulphur-terminated edges confined in a SWCNT; grey: carbon, yellow: sulphur. (b), (d), (e), (f) Adapted by permission from Macmillan Publishers Ltd: *Nature Materials* (ref. 278), Copyright (2011).

IV. Conclusions and outlook

Recent advancements in the chemical synthesis of nanographenes with newly developed "non-conventional" methods have vastly expanded the scope of available graphene molecules, including a variety of symmetries, configurations, embedded seven- or eight-membered rings, heteroatom doping, and edge functionalization. The synthesis was further extended to the longitudinally extended polymeric systems, providing access to structurally well-defined GNRs with varying configurations, *i.e.*, different widths, lengths, edge structures and selectively doped heteroatoms. Precise GNR synthesis has been achieved using both the conventional solution-mediated method and the modern surface-based approach under UHV conditions. The structural variations in graphene molecules and GNRs have allowed fine-tuning of their (opto-)electronic properties, which would be the basis for the future application of such nanocarbon materials.

In particular, heteroatom doping was found to be an effective strategy modulating the electronic properties of graphene molecules and GNRs. Heteroatom doping in different structures with varying doping positions and concentrations, as well as the incorporation of other main group elements beyond the examples summarized above, would further enrich their chemistry. Particularly, further developments of B-, BN- and P-doped graphene molecules, as well as syntheses of silicon (Si)-, germanium (Ge)- and selenium (Se)-doped graphene molecules are awaited. Regarding GNRs, the fabrication of N-doped structures with different configurations and doping concentrations and the preparation of S-, B-, or BN-doped analogues will be an important next step. Pushing the limit of the size and doping concentration will not only provide new materials with interesting properties but also enable elucidation of the fundamental structure–property relationships of heteroatom-doped graphene molecules and GNRs.

Although most of the GNRs synthesized to date feature, in principle, armchair edge structures, GNRs with a zigzag edge configuration are predicted to show localized edge states that can be spin polarized, and thus these GNRs are interesting for spintronic applications.[27–29] We have been working on the surface-assisted synthesis of partial and full zigzag GNRs and

have obtained positive indications that such GNRs indeed possess localized states at the edges.

In addition to heteroatom doping and the zigzag edge configuration, further major challenges in the synthesis of GNRs include (1) obtaining GNRs with different widths, particularly lateral extension over 3 nm to achieve a bandgap smaller than 1 eV; (2) incorporating non-six-membered rings, such as five-, seven- or eight-membered rings, which will also serve as models of grain boundaries in graphene; (3) structurally distorting GNRs in similar manners to contorted graphene molecules; (4) achieving greater control in fabricating GNR heterojunctions or block copolymers to form longer "blocks" and (5) functionalizing the GNR edges and/or terminals, for example, to tune the energy levels with electron-donating/-withdrawing groups or to enhance the affinity to desired substrates or electrode materials. These are all important challenges for the future nanoelectronic and optoelectronic applications of such nanographene materials.

Acknowledgements

We acknowledge all of our distinguished partner groups and dedicated associates, who enabled our contributions to the achievements described in this article. We thank the financial support by EU Projects GENIUS (ITN-264694), UPGRADE and MoQuaS, ERC-Adv.-Grant 267160 (NANOGRAPH), Graphene Flagship (No. CNECT-ICT-604391), the Office of Naval Research BRC Program (molecular synthesis and characterization) and DFG Priority Program SPP 1459. We are also thankful to fruitful collaborations with BASF SE, Ludwigshafen.

Notes and references

1 K. S. Novoselov, A. K. Geim, S. V. Morozov, D. Jiang, Y. Zhang, S. V. Dubonos, I. V. Grigorieva and A. A. Firsov, *Science*, 2004, **306**, 666.
2 A. K. Geim and K. S. Novoselov, *Nat. Mater.*, 2007, **6**, 183.
3 R. F. Service, *Science*, 2009, **324**, 875.
4 K. S. Novoselov, V. I. Falko, L. Colombo, P. R. Gellert, M. G. Schwab and K. Kim, *Nature*, 2012, **490**, 192.
5 F. Schwierz, *Nat. Nanotechnol.*, 2010, **5**, 487.
6 R. Rieger and K. Müllen, *J. Phys. Org. Chem.*, 2010, **23**, 315.
7 M. Bacon, S. J. Bradley and T. Nann, *Part. Part. Syst. Charact.*, 2014, **31**, 415.
8 S. Kim, S. W. Hwang, M.-K. Kim, D. Y. Shin, D. H. Shin, C. O. Kim, S. B. Yang, J. H. Park, E. Hwang, S.-H. Choi, G. Ko, S. Sim, C. Sone, H. J. Choi, S. Bae and B. H. Hong, *ACS Nano*, 2012, **6**, 8203.
9 J. Wu, W. Pisula and K. Müllen, *Chem. Rev.*, 2007, **107**, 718.
10 K. Müllen, *ACS Nano*, 2014, **8**, 6531.
11 R. Scholl and C. Seer, *Liebigs Ann. Chem.*, 1912, **394**, 111.
12 R. Scholl and C. Seer, *Chem. Ber.*, 1922, **55**, 330.
13 R. Scholl, C. Seer and R. Weitzenböck, *Chem. Ber.*, 1910, **43**, 2202.
14 E. Clar and J. F. Stephen, *Tetrahedron*, 1965, **21**, 467.
15 E. Clar and W. schmidt, *Tetrahedron*, 1979, **35**, 2673.
16 E. Clar and D. G. Stewart, *J. Am. Chem. Soc.*, 1953, **75**, 2667.
17 L. Chen, Y. Hernandez, X. Feng and K. Müllen, *Angew. Chem., Int. Ed.*, 2012, **51**, 7640.
18 X. Yan and L.-s. Li, *J. Mater. Chem.*, 2011, **21**, 3295.
19 K. K. Baldridge and J. S. Siegel, *Angew. Chem., Int. Ed.*, 2013, **52**, 5436.
20 M. Ball, Y. Zhong, Y. Wu, C. Schenck, F. Ng, M. Steigerwald, S. Xiao and C. Nuckolls, *Acc. Chem. Res.*, 2015, **48**, 267.
21 W. Pisula, X. L. Feng and K. Müllen, *Chem. Mater.*, 2011, **23**, 554.
22 Y. Morita, S. Suzuki, K. Sato and T. Takui, *Nat. Chem.*, 2011, **3**, 197.
23 Z. Sun, Z. Zeng and J. Wu, *Chem. – Asian J.*, 2013, **8**, 2894.
24 X. Li, X. Wang, L. Zhang, S. Lee and H. Dai, *Science*, 2008, **319**, 1229.
25 A. Narita, X. Feng and K. Müllen, *Chem. Rec.*, 2015, **15**, 295.
26 O. V. Yazyev, *Acc. Chem. Res.*, 2013, **46**, 2319.
27 M. Terrones, A. R. Botello-Méndez, J. Campos-Delgado, F. López-Urías, Y. I. Vega-Cantú, F. J. Rodríguez-Macías, A. L. Elías, E. Muñoz-Sandoval, A. G. Cano-Márquez, J.-C. Charlier and H. Terrones, *Nano Today*, 2010, **5**, 351.
28 Y. W. Son, M. L. Cohen and S. G. Louie, *Nature*, 2006, **444**, 347.
29 O. V. Yazyev, *Rep. Prog. Phys.*, 2010, **73**, 056501.
30 W. Y. Kim and K. S. Kim, *Nat. Nanotechnol.*, 2008, **3**, 408.
31 X.-R. Wang, Y. Shi and R. Zhang, *Chin. Phys. B*, 2013, **22**, 098505.
32 M. Han, B. Özyilmaz, Y. Zhang and P. Kim, *Phys. Rev. Lett.*, 2007, **98**, 206805.
33 Z. Chen, Y. Lin, M. Rooks and P. Avouris, *Physica E*, 2007, **40**, 228.
34 L. Tapaszto, G. Dobrik, P. Lambin and L. P. Biro, *Nat. Nanotechnol.*, 2008, **3**, 397.
35 D. V. Kosynkin, A. L. Higginbotham, A. Sinitskii, J. R. Lomeda, A. Dimiev, B. K. Price and J. M. Tour, *Nature*, 2009, **458**, 872.
36 L. Jiao, L. Zhang, X. Wang, G. Diankov and H. Dai, *Nature*, 2009, **458**, 877.
37 J. Cai, P. Ruffieux, R. Jaafar, M. Bieri, T. Braun, S. Blankenburg, M. Muoth, A. P. Seitsonen, M. Saleh, X. Feng, K. Müllen and R. Fasel, *Nature*, 2010, **466**, 470.
38 J. Cai, C. A. Pignedoli, L. Talirz, P. Ruffieux, H. Söde, L. Liang, V. Meunier, R. Berger, R. Li, X. Feng, K. Müllen and R. Fasel, *Nat. Nanotechnol.*, 2014, **9**, 896.
39 Y.-C. Chen, T. Cao, C. Chen, Z. Pedramrazi, D. Haberer, D. G. de Oteyza, F. R. Fischer, S. G. Louie and M. F. Crommie, *Nat. Nanotechnol.*, 2015, **10**, 156.
40 M. D. Watson, A. Fechtenkötter and K. Müllen, *Chem. Rev.*, 2001, **101**, 1267.
41 W. Jiang, Y. Li and Z. Wang, *Chem. Soc. Rev.*, 2013, **42**, 6113.
42 B. Schmaltz, T. Weil and K. Müllen, *Adv. Mater.*, 2009, **21**, 1067.
43 Y. Segawa, T. Maekawa and K. Itami, *Angew. Chem., Int. Ed.*, 2015, **54**, 66.
44 A. Sygula, *Eur. J. Org. Chem.*, 2011, 1611.
45 D. Wu, H. Ge, S. H. Liu and J. Yin, *RSC Adv.*, 2013, **3**, 22727.

46 Z. Sun, Q. Ye, C. Chi and J. Wu, *Chem. Soc. Rev.*, 2012, **41**, 7857.
47 Y. Tobe, *Chem. Rec.*, 2015, **15**, 86.
48 V. M. Tsefrikas and L. T. Scott, *Chem. Rev.*, 2006, **106**, 4868.
49 Z. Sun, Z. Zeng and J. Wu, *Acc. Chem. Res.*, 2014, **47**, 2582.
50 Z. Sun and J. Wu, *J. Mater. Chem.*, 2012, **22**, 4151.
51 T. Kubo, *Chem. Lett.*, 2015, **44**, 111.
52 T. Kubo, *Chem. Rec.*, 2015, **15**, 218.
53 A. Konishi, Y. Hirao, H. Kurata, T. Kubo, M. Nakano and K. Kamada, *Pure Appl. Chem.*, 2014, **86**, 497.
54 T. Amaya and T. Hirao, *Chem. Rec.*, 2015, **15**, 310.
55 M. Mojica, J. A. Alonso and F. Méndez, *J. Phys. Org. Chem.*, 2013, **26**, 526.
56 T. Jin, J. Zhao, N. Asao and Y. Yamamoto, *Chem. – Eur. J.*, 2014, **20**, 3554.
57 B. M. Schmidt and D. Lentz, *Chem. Lett.*, 2014, **43**, 171.
58 H. F. Bettinger and C. Tönshoff, *Chem. Rec.*, 2015, **15**, 364.
59 M. Watanabe, K.-Y. Chen, Y. J. Chang and T. J. Chow, *Acc. Chem. Res.*, 2013, **46**, 1606.
60 A. Mateo-Alonso, *Chem. Soc. Rev.*, 2014, **43**, 6311.
61 U. H. F. Bunz, J. U. Engelhart, B. D. Lindner and M. Schaffroth, *Angew. Chem., Int. Ed.*, 2013, **52**, 3810.
62 L. Chen, C. Li and K. Müllen, *J. Mater. Chem. C*, 2014, **2**, 1938.
63 W. Jiang, Y. Li and Z. Wang, *Acc. Chem. Res.*, 2014, **47**, 3135.
64 N. Saleh, C. Shen and J. Crassous, *Chem. Sci.*, 2014, **5**, 3680.
65 M. Gingras, *Chem. Soc. Rev.*, 2013, **42**, 968.
66 M. Gingras, G. Felix and R. Peresutti, *Chem. Soc. Rev.*, 2013, **42**, 1007.
67 M. Gingras, *Chem. Soc. Rev.*, 2013, **42**, 1051.
68 Y. Shen and C.-F. Chen, *Chem. Rev.*, 2012, **112**, 1463.
69 K. Shi, J.-Y. Wang and J. Pei, *Chem. Rec.*, 2015, **15**, 52.
70 H. Zhang, D. Wu, S. Hua Liu and J. Yin, *Curr. Org. Chem.*, 2012, **16**, 2124.
71 M. Grzybowski, K. Skonieczny, H. Butenschön and D. T. Gryko, *Angew. Chem., Int. Ed.*, 2013, **52**, 9900.
72 R. Dorel, C. Manzano, M. Grisolia, W.-H. Soe, C. Joachim and A. M. Echavarren, *Chem. Commun.*, 2015, **51**, 6932.
73 A. Matsumoto, M. Suzuki, D. Kuzuhara, H. Hayashi, N. Aratani and H. Yamada, *Angew. Chem., Int. Ed.*, 2015, **54**, 8175.
74 C. D. Simpson, J. D. Brand, A. J. Berresheim, L. Przybilla, H. J. Räder and K. Müllen, *Chem. – Eur. J.*, 2002, **8**, 1424.
75 A. A. Sarhan and C. Bolm, *Chem. Soc. Rev.*, 2009, **38**, 2730.
76 S. R. Waldvogel and S. Trosien, *Chem. Commun.*, 2012, **48**, 9109.
77 L. Zhai, R. Shukla and R. Rathore, *Org. Lett.*, 2009, **11**, 3474.
78 B. T. King, J. Kroulík, C. R. Robertson, P. Rempala, C. L. Hilton, J. D. Korinek and L. M. Gortari, *J. Org. Chem.*, 2007, **72**, 2279.
79 F. Morgenroth, C. Kübel, M. Müller, U. M. Wiesler, A. J. Berresheim, M. Wagner and K. Müllen, *Carbon*, 1998, **36**, 833.
80 J. L. Ormsby, T. D. Black, C. L. Hilton, Bharat and B. T. King, *Tetrahedron*, 2008, **64**, 11370.
81 F. Dötz, J. D. Brand, S. Ito, L. Gherghel and K. Müllen, *J. Am. Chem. Soc.*, 2000, **122**, 7707.
82 K. Yoshimura, L. Przybilla, S. Ito, J. D. Brand, M. Wehmeir, H. J. Räder and K. Müllen, *Macromol. Chem. Phys.*, 2001, **202**, 215.
83 X. Dou, X. Yang, G. J. Bodwell, M. Wagner, V. Enkelmann and K. Müllen, *Org. Lett.*, 2007, **9**, 2485.
84 H. Arslan, F. J. Uribe-Romo, B. J. Smith and W. R. Dichtel, *Chem. Sci.*, 2013, **4**, 3973.
85 A. C. Whalley, K. N. Plunkett, A. A. Gorodetsky, C. L. Schenck, C.-Y. Chiu, M. L. Steigerwald and C. Nuckolls, *Chem. Sci.*, 2011, **2**, 132.
86 S. J. Hein, H. Arslan, I. Keresztes and W. R. Dichtel, *Org. Lett.*, 2014, **16**, 4416.
87 H. Arslan, J. D. Saathoff, D. N. Bunck, P. Clancy and W. R. Dichtel, *Angew. Chem., Int. Ed.*, 2012, **51**, 12051.
88 Q. Zhang, H. Peng, G. Zhang, Q. Lu, J. Chang, Y. Dong, X. Shi and J. Wei, *J. Am. Chem. Soc.*, 2014, **136**, 5057.
89 A. A. Gorodetsky, C.-Y. Chiu, T. Schiros, M. Palma, M. Cox, Z. Jia, W. Sattler, I. Kymissis, M. Steigerwald and C. Nuckolls, *Angew. Chem., Int. Ed.*, 2010, **49**, 7909.
90 C.-Y. Chiu, B. Kim, A. A. Gorodetsky, W. Sattler, S. Wei, A. Sattler, M. Steigerwald and C. Nuckolls, *Chem. Sci.*, 2011, **2**, 1480.
91 L. Chen, S. R. Puniredd, Y.-Z. Tan, M. Baumgarten, U. Zschieschang, V. Enkelmann, W. Pisula, X. Feng, H. Klauk and K. Müllen, *J. Am. Chem. Soc.*, 2012, **134**, 17869.
92 L. Chen, K. S. Mali, S. R. Puniredd, M. Baumgarten, K. Parvez, W. Pisula, S. De Feyter and K. Müllen, *J. Am. Chem. Soc.*, 2013, **135**, 13531.
93 D. Pérez, D. Peña and E. Guitián, *Eur. J. Org. Chem.*, 2013, 5981.
94 D. Peña, S. Escudero, D. Pérez, E. Guitián and L. Castedo, *Angew. Chem., Int. Ed.*, 1998, **37**, 2659.
95 D. Peña, D. Pérez, E. Guitián and L. Castedo, *Org. Lett.*, 1999, **1**, 1555.
96 C. Romero, D. Peña, D. Pérez and E. Guitián, *Chem. – Eur. J.*, 2006, **12**, 5677.
97 J. M. Alonso, A. E. Díaz-Álvarez, A. Criado, D. Pérez, D. Peña and E. Guitián, *Angew. Chem., Int. Ed.*, 2012, **51**, 173.
98 B. Schuler, S. Collazos, L. Gross, G. Meyer, D. Pérez, E. Guitián and D. Peña, *Angew. Chem., Int. Ed.*, 2014, **53**, 9004.
99 Z.-H. Zhou and T. Yamamoto, *J. Organomet. Chem.*, 1991, **414**, 119.
100 E. C. Rüdiger, M. Porz, M. Schaffroth, F. Rominger and U. H. F. Bunz, *Chem. – Eur. J.*, 2014, **20**, 12725.
101 M. Shimizu and T. Hiyama, *Eur. J. Org. Chem.*, 2013, 8069.
102 C.-N. Feng, Y.-C. Hsieh and Y.-T. Wu, *Chem. Rec.*, 2015, **15**, 266.
103 D. M. Hitt and J. M. O'Connor, *Chem. Rev.*, 2011, **111**, 7904.
104 K. Y. Amsharov, M. A. Kabdulov and M. Jansen, *Angew. Chem., Int. Ed.*, 2012, **51**, 4594.
105 K. Y. Amsharov and P. Merz, *J. Org. Chem.*, 2012, **77**, 5445.
106 T.-A. Chen and R.-S. Liu, *Chem. – Eur. J.*, 2011, **17**, 8023.
107 T.-A. Chen and R.-S. Liu, *Org. Lett.*, 2011, **13**, 4644.
108 J. Liu, B.-W. Li, Y.-Z. Tan, A. Giannakopoulos, C. Sanchez-Sanchez, D. Beljonne, P. Ruffieux, R. Fasel, X. Feng and K. Müllen, *J. Am. Chem. Soc.*, 2015, **137**, 6097.

109 Q. Yan, K. Cai, C. Zhang and D. Zhao, *Org. Lett.*, 2012, **14**, 4654.
110 C.-W. Li, C.-I. Wang, H.-Y. Liao, R. Chaudhuri and R.-S. Liu, *J. Org. Chem.*, 2007, **72**, 9203.
111 C. Thilgen, *Angew. Chem., Int. Ed.*, 2012, **51**, 7082.
112 H. Ohno, *Asian J. Org. Chem.*, 2013, **2**, 18.
113 P. Y. Huang, C. S. Ruiz-Vargas, A. M. van der Zande, W. S. Whitney, M. P. Levendorf, J. W. Kevek, S. Garg, J. S. Alden, C. J. Hustedt, Y. Zhu, J. Park, P. L. McEuen and D. A. Muller, *Nature*, 2011, **469**, 389.
114 K. Kim, Z. Lee, W. Regan, C. Kisielowski, M. F. Crommie and A. Zettl, *ACS Nano*, 2011, **5**, 2142.
115 S. Kurasch, J. Kotakoski, O. Lehtinen, V. Skákalová, J. Smet, C. E. Krill, A. V. Krasheninnikov and U. Kaiser, *Nano Lett.*, 2012, **12**, 3168.
116 J. Lahiri, Y. Lin, P. Bozkurt, I. I. Oleynik and M. Batzill, *Nat. Nanotechnol.*, 2010, **5**, 326.
117 P. B. László and L. Philippe, *New J. Phys.*, 2013, **15**, 035024.
118 Y.-T. Wu and J. S. Siegel, *Chem. Rev.*, 2006, **106**, 4843.
119 K. Yamamoto and H. Matsubara, *J. Synth. Org. Chem., Jpn.*, 1995, **53**, 318.
120 J. H. Dopper and H. Wynberg, *Tetrahedron Lett.*, 1972, **13**, 763.
121 T. J. Seiders and J. S. Siegel, *Chem. Br.*, 1995, **31**, 313.
122 K. Yamamoto, T. Harada, M. Nakazaki, T. Naka, Y. Kai, S. Harada and N. Kasai, *J. Am. Chem. Soc.*, 1983, **105**, 7171.
123 K. Yamamoto, Y. Saitho, D. Iwaki and T. Ooka, *Angew. Chem., Int. Ed. Engl.*, 1991, **30**, 1173.
124 J. Luo, X. Xu, R. Mao and Q. Miao, *J. Am. Chem. Soc.*, 2012, **134**, 13796.
125 K. Y. Cheung, X. Xu and Q. Miao, *J. Am. Chem. Soc.*, 2015, **137**, 3910.
126 A. Pradhan, P. Dechambenoit, H. Bock and F. Durola, *J. Org. Chem.*, 2013, **78**, 2266.
127 K. Kawasumi, Q. Zhang, Y. Segawa, L. T. Scott and K. Itami, *Nat. Chem.*, 2013, **5**, 739.
128 Q. Zhang, K. Kawasumi, Y. Segawa, K. Itami and L. T. Scott, *J. Am. Chem. Soc.*, 2012, **134**, 15664.
129 K. Mochida, K. Kawasumi, Y. Segawa and K. Itami, *J. Am. Chem. Soc.*, 2011, **133**, 10716.
130 R. Salcedo, L. E. Sansores, A. Picazo and L. Sansón, *THEOCHEM*, 2004, **678**, 211.
131 B. Thulin and O. Wennerström, *Acta Chem. Scand., Ser. B*, 1976, **30**, 369.
132 C.-N. Feng, M.-Y. Kuo and Y.-T. Wu, *Angew. Chem., Int. Ed.*, 2013, **52**, 7791.
133 Y. Sakamoto and T. Suzuki, *J. Am. Chem. Soc.*, 2013, **135**, 14074.
134 R. W. Miller, A. K. Duncan, S. T. Schneebeli, D. L. Gray and A. C. Whalley, *Chem. – Eur. J.*, 2014, **20**, 3705.
135 F. Schlütter, T. Nishiuchi, V. Enkelmann and K. Müllen, *Angew. Chem., Int. Ed.*, 2014, **53**, 1538.
136 X. Wang, G. Sun, P. Routh, D.-H. Kim, W. Huang and P. Chen, *Chem. Soc. Rev.*, 2014, **43**, 7067.
137 U. N. Maiti, W. J. Lee, J. M. Lee, Y. Oh, J. Y. Kim, J. E. Kim, J. Shim, T. H. Han and S. O. Kim, *Adv. Mater.*, 2014, **26**, 40.
138 H. T. Liu, Y. Q. Liu and D. B. Zhu, *J. Mater. Chem.*, 2011, **21**, 3335.
139 X.-Y. Wang, J.-Y. Wang and J. Pei, *Chem. – Eur. J.*, 2015, **21**, 3528.
140 P. G. Campbell, A. J. V. Marwitz and S. Y. Liu, *Angew. Chem., Int. Ed.*, 2012, **51**, 6074.
141 M. J. D. Bosdet and W. E. Piers, *Can. J. Chem.*, 2009, **87**, 8.
142 M. Takase, V. Enkelmann, D. Sebastiani, M. Baumgarten and K. Müllen, *Angew. Chem., Int. Ed.*, 2007, **46**, 5524.
143 M. Takase, T. Narita, W. Fujita, M. S. Asano, T. Nishinaga, H. Benten, K. Yoza and K. Müllen, *J. Am. Chem. Soc.*, 2013, **135**, 8031.
144 H. Uoyama, K. Goushi, K. Shizu, H. Nomura and C. Adachi, *Nature*, 2012, **492**, 234.
145 E. Gońka, P. J. Chmielewski, T. Lis and M. Stępień, *J. Am. Chem. Soc.*, 2014, **136**, 16399.
146 S. M. Draper, D. J. Gregg and R. Madathil, *J. Am. Chem. Soc.*, 2002, **124**, 3486.
147 S. M. Draper, D. J. Gregg, E. R. Schofield, W. R. Browne, M. Duati, J. G. Vos and P. Passaniti, *J. Am. Chem. Soc.*, 2004, **126**, 8694.
148 L. P. Wijesinghe, B. S. Lankage, G. M. O. Maille, S. D. Perera, D. Nolan, L. Wang and S. M. Draper, *Chem. Commun.*, 2014, **50**, 10637.
149 J. F. Wei, B. Han, Q. A. Guo, X. Y. Shi, W. L. Wang and N. Wei, *Angew. Chem., Int. Ed.*, 2010, **49**, 8209.
150 B. He, A. B. Pun, L. M. Klivansky, A. M. McGough, Y. Ye, J. Zhu, J. Guo, S. J. Teat and Y. Liu, *Chem. Mater.*, 2014, **26**, 3920.
151 R. Berger, A. Giannakopoulos, P. Ravat, M. Wagner, D. Beljonne, X. Feng and K. Müllen, *Angew. Chem., Int. Ed.*, 2014, **53**, 10520.
152 R. Berger, M. Wagner, X. Feng and K. Müllen, *Chem. Sci.*, 2015, **6**, 436.
153 S. Ito, Y. Tokimaru and K. Nozaki, *Chem. Commun.*, 2015, **51**, 221.
154 S. Ito, Y. Tokimaru and K. Nozaki, *Angew. Chem., Int. Ed.*, 2015, **54**, 7256.
155 S. C. Gadekar, B. K. Reddy and V. G. Anand, *Chem. Commun.*, 2015, **51**, 8342.
156 K. Skonieczny and D. T. Gryko, *J. Org. Chem.*, 2015, **80**, 5753.
157 M. E. Cinar and T. Ozturk, *Chem. Rev.*, 2015, **115**, 3036.
158 K. Takimiya, I. Osaka, T. Mori and M. Nakano, *Acc. Chem. Res.*, 2014, **47**, 1493.
159 Y. Cao, X.-Y. Wang, J.-Y. Wang and J. Pei, *Synlett*, 2014, 313.
160 K. Y. Chernichenko, V. V. Sumerin, R. V. Shpanchenko, E. S. Balenkova and V. G. Nenajdenko, *Angew. Chem., Int. Ed.*, 2006, **45**, 7367.
161 L. Zou, X.-Y. Wang, K. Shi, J.-Y. Wang and J. Pei, *Org. Lett.*, 2013, **15**, 4378.
162 H. Oshima, A. Fukazawa, T. Sasamori and S. Yamaguchi, *Angew. Chem., Int. Ed.*, 2015, **54**, 7636.
163 R.-Q. Lu, Y.-N. Zhou, X.-Y. Yan, K. Shi, Y.-Q. Zheng, M. Luo, X.-C. Wang, J. Pei, H. Xia, L. Zoppi, K. K. Baldridge, J. S. Siegel and X.-Y. Cao, *Chem. Commun.*, 2015, **51**, 1681.

164 X. Feng, J. Wu, M. Ai, W. Pisula, L. Zhi, J. P. Rabe and K. Müllen, *Angew. Chem., Int. Ed.*, 2007, **46**, 3033.
165 C. J. Martin, B. Gil, S. D. Perera and S. M. Draper, *Chem. Commun.*, 2011, **47**, 3616.
166 S. J. Kang, J. B. Kim, C.-Y. Chiu, S. Ahn, T. Schiros, S. S. Lee, K. G. Yager, M. F. Toney, Y.-L. Loo and C. Nuckolls, *Angew. Chem., Int. Ed.*, 2012, **51**, 8594.
167 A. Escande and M. J. Ingleson, *Chem. Commun.*, 2015, **51**, 6257.
168 Z. Zhou, A. Wakamiya, T. Kushida and S. Yamaguchi, *J. Am. Chem. Soc.*, 2012, **134**, 4529.
169 S. Saito, K. Matsuo and S. Yamaguchi, *J. Am. Chem. Soc.*, 2012, **134**, 9130.
170 C. Dou, S. Saito, K. Matsuo, I. Hisaki and S. Yamaguchi, *Angew. Chem., Int. Ed.*, 2012, **51**, 12206.
171 K. Matsuo, S. Saito and S. Yamaguchi, *J. Am. Chem. Soc.*, 2014, **136**, 12580.
172 V. M. Hertz, M. Bolte, H.-W. Lerner and M. Wagner, *Angew. Chem., Int. Ed.*, 2015, DOI: 10.1002/anie.201502977.
173 X.-Y. Wang, H.-R. Lin, T. Lei, D.-C. Yang, F.-D. Zhuang, J.-Y. Wang, S.-C. Yuan and J. Pei, *Angew. Chem., Int. Ed.*, 2013, **52**, 3117.
174 X.-Y. Wang, F.-D. Zhuang, X. Zhou, D.-C. Yang, J.-Y. Wang and J. Pei, *J. Mater. Chem. C*, 2014, **2**, 8152.
175 J. S. A. Ishibashi, J. L. Marshall, A. Mazière, G. J. Lovinger, B. Li, L. N. Zakharov, A. Dargelos, A. Graciaa, A. Chrostowska and S.-Y. Liu, *J. Am. Chem. Soc.*, 2014, **136**, 15414.
176 B. Neue, J. F. Araneda, W. E. Piers and M. Parvez, *Angew. Chem., Int. Ed.*, 2013, **52**, 9966.
177 X. Wang, F. Zhang, J. Liu, R. Z. Tang, Y. B. Fu, D. Q. Wu, Q. Xu, X. D. Zhuang, G. F. He and X. L. Feng, *Org. Lett.*, 2013, **15**, 5714.
178 T. Hatakeyama, S. Hashimoto, S. Seki and M. Nakamura, *J. Am. Chem. Soc.*, 2011, **133**, 18614.
179 M. J. D. Bosdet, W. E. Piers, T. S. Sorensen and M. Parvez, *Angew. Chem., Int. Ed.*, 2007, **46**, 4940.
180 D. J. H. Emslie, W. E. Piers and M. Parvez, *Angew. Chem., Int. Ed.*, 2003, **42**, 1252.
181 X.-Y. Wang, F.-D. Zhuang, R.-B. Wang, X.-C. Wang, X.-Y. Cao, J.-Y. Wang and J. Pei, *J. Am. Chem. Soc.*, 2014, **136**, 3764.
182 X.-Y. Wang, F.-D. Zhuang, X.-C. Wang, X.-Y. Cao, J.-Y. Wang and J. Pei, *Chem. Commun.*, 2015, **51**, 4368.
183 G. Li, W.-W. Xiong, P.-Y. Gu, J. Cao, J. Zhu, R. Ganguly, Y. Li, A. C. Grimsdale and Q. Zhang, *Org. Lett.*, 2015, **17**, 560.
184 D. Wu, H. Zhang, J. Liang, H. Ge, C. Chi, J. Wu, S. H. Liu and J. Yin, *J. Org. Chem.*, 2012, **77**, 11319.
185 M. Krieg, F. Reicherter, P. Haiss, M. Ströbele, K. Eichele, M.-J. Treanor, R. Schaub and H. F. Bettinger, *Angew. Chem., Int. Ed.*, 2015, **54**, 8284.
186 Y. Matano and H. Imahori, *Org. Biomol. Chem.*, 2009, **7**, 1258.
187 T. Baumgartner and R. Réau, *Chem. Rev.*, 2006, **106**, 4681.
188 M. Stolar and T. Baumgartner, *Chem. – Asian J.*, 2014, **9**, 1212.
189 T. Hatakeyama, S. Hashimoto and M. Nakamura, *Org. Lett.*, 2011, **13**, 2130.
190 S. Hashimoto, S. Nakatsuka, M. Nakamura and T. Hatakeyama, *Angew. Chem., Int. Ed.*, 2014, **53**, 14074.
191 P.-A. Bouit, A. Escande, R. Szűcs, D. Szieberth, C. Lescop, L. Nyulászi, M. Hissler and R. Réau, *J. Am. Chem. Soc.*, 2012, **134**, 6524.
192 S. Sergeyev, W. Pisula and Y. H. Geerts, *Chem. Soc. Rev.*, 2007, **36**, 1902.
193 S. Ito, M. Wehmeier, J. D. Brand, C. Kübel, R. Epsch, J. P. Rabe and K. Müllen, *Chem. – Eur. J.*, 2000, **6**, 4327.
194 L. Chen, X. Dou, W. Pisula, X. Y. Yang, D. Q. Wu, G. Floudas, X. L. Feng and K. Müllen, *Chem. Commun.*, 2012, **48**, 702.
195 J. Wu, A. Fechtenkötter, J. Gauss, M. D. Watson, M. Kastler, C. Fechtenkötter, M. Wagner and K. Müllen, *J. Am. Chem. Soc.*, 2004, **126**, 11311.
196 L. F. Dössel, V. Kamm, I. A. Howard, F. Laquai, W. Pisula, X. Feng, C. Li, M. Takase, T. Kudernac, S. De Feyter and K. Müllen, *J. Am. Chem. Soc.*, 2012, **134**, 5876.
197 P. Ravat, T. Marszalek, W. Pisula, K. Müllen and M. Baumgarten, *J. Am. Chem. Soc.*, 2014, **136**, 12860.
198 Y.-Z. Tan, B. Yang, K. Parvez, A. Narita, S. Osella, D. Beljonne, X. Feng and K. Müllen, *Nat. Commun.*, 2013, **4**, 2646.
199 C. L. Hilton, J. M. Crowfoot, P. Rempala and B. T. King, *J. Am. Chem. Soc.*, 2008, **130**, 13392.
200 Y.-Z. Tan, S. Osella, Y. Liu, B. Yang, D. Beljonne, X. Feng and K. Müllen, *Angew. Chem., Int. Ed.*, 2015, **54**, 2927.
201 I. A. I. Mkhalid, J. H. Barnard, T. B. Marder, J. M. Murphy and J. F. Hartwig, *Chem. Rev.*, 2009, **110**, 890.
202 R. Yamaguchi, S. Hiroto and H. Shinokubo, *Org. Lett.*, 2012, **14**, 2472.
203 H. Shinokubo, *Proc. Jpn. Acad., Ser. B*, 2014, **90**, 1.
204 R. Yamaguchi, S. Ito, B. S. Lee, S. Hiroto, D. Kim and H. Shinokubo, *Chem. – Asian J.*, 2013, **8**, 178.
205 K. Takagi and Y. Sakakibara, *Chem. Lett.*, 1989, 1957.
206 K. Ozaki, K. Kawasumi, M. Shibata, H. Ito and K. Itami, *Nat. Commun.*, 2015, **6**, 6251.
207 M. N. Eliseeva and L. T. Scott, *J. Am. Chem. Soc.*, 2012, **134**, 15169.
208 E. H. Fort, P. M. Donovan and L. T. Scott, *J. Am. Chem. Soc.*, 2009, **131**, 16006.
209 E. H. Fort and L. T. Scott, *Angew. Chem., Int. Ed.*, 2010, **49**, 6626.
210 E. H. Fort and L. T. Scott, *Tetrahedron Lett.*, 2011, **52**, 2051.
211 J. Li, C. Jiao, K.-W. Huang and J. Wu, *Chem. – Eur. J.*, 2011, **17**, 14672.
212 E. H. Fort, M. S. Jeffreys and L. T. Scott, *Chem. Commun.*, 2012, **48**, 8102.
213 A. Konishi, Y. Hirao, K. Matsumoto, H. Kurata and T. Kubo, *Chem. Lett.*, 2013, **42**, 592.
214 J. K. Stille, G. K. Noren and L. Green, *J. Polym. Sci., Part A-1: Polym. Chem.*, 1970, **8**, 2245.
215 A. D. Schlüter, M. Löffler and V. Enkelmann, *Nature*, 1994, **368**, 831.

216 M. Löffler, A.-D. Schlüter, K. Gessler, W. Saenger, J.-M. Toussaint and J.-L. Brédas, *Angew. Chem., Int. Ed. Engl.*, 1994, **33**, 2209.
217 K. Chmil and U. Scherf, *Makromol. Chem., Rapid Commun.*, 1993, **14**, 217.
218 K. Chmil and U. Scherf, *Acta Polym.*, 1997, **48**, 208.
219 U. Scherf, *J. Mater. Chem.*, 1999, **9**, 1853.
220 M. B. Goldfinger and T. M. Swager, *J. Am. Chem. Soc.*, 1994, **116**, 7895.
221 Z. B. Shifrina, M. S. Averina, A. L. Rusanov, M. Wagner and K. Müllen, *Macromolecules*, 2000, **33**, 3525.
222 J. S. Wu, L. Gherghel, M. D. Watson, J. X. Li, Z. H. Wang, C. D. Simpson, U. Kolb and K. Müllen, *Macromolecules*, 2003, **36**, 7082.
223 T. Ikeda, N. Aratani and A. Osuka, *Chem. – Asian J.*, 2009, **4**, 1248.
224 T. Tanaka and A. Osuka, *Chem. Soc. Rev.*, 2015, **44**, 943.
225 A. Tsuda and A. Osuka, *Science*, 2001, **293**, 79.
226 A. Tsuda, H. Furuta and A. Osuka, *Angew. Chem., Int. Ed.*, 2000, **39**, 2549.
227 X. Y. Yang, X. Dou, A. Rouhanipour, L. J. Zhi, H. J. Rader and K. Müllen, *J. Am. Chem. Soc.*, 2008, **130**, 4216.
228 L. Dössel, L. Gherghel, X. Feng and K. Müllen, *Angew. Chem., Int. Ed.*, 2011, **50**, 2540.
229 A. Narita, X. Feng, Y. Hernandez, S. A. Jensen, M. Bonn, H. Yang, I. A. Verzhbitskiy, C. Casiraghi, M. R. Hansen, A. H. R. Koch, G. Fytas, O. Ivasenko, B. Li, K. S. Mali, T. Balandina, S. Mahesh, S. De Feyter and K. Müllen, *Nat. Chem.*, 2014, **6**, 126.
230 K. T. Kim, J. W. Jung and W. H. Jo, *Carbon*, 2013, **63**, 202.
231 K. T. Kim, J. W. Lee and W. H. Jo, *Macromol. Chem. Phys.*, 2013, **214**, 2768.
232 M. G. Schwab, A. Narita, S. Osella, Y. Hu, A. Maghsoumi, A. Mavrinsky, W. Pisula, C. Castiglioni, M. Tommasini, D. Beljonne, X. Feng and K. Müllen, *Chem. – Asian J.*, 2015, DOI: 10.1002/asia.201500450.
233 W. H. Carothers, *Trans. Faraday Soc.*, 1936, **32**, 39.
234 G. G. Odian, *Principles of Polymerization*, J. Wiley & Sons, Hoboken, NJ, 2004.
235 S. Setayesh, A. C. Grimsdale, T. Weil, V. Enkelmann, K. Müllen, F. Meghdadi, E. J. W. List and G. Leising, *J. Am. Chem. Soc.*, 2001, **123**, 946.
236 J. Lee, H.-J. Cho, B.-J. Jung, N. S. Cho and H.-K. Shim, *Macromolecules*, 2004, **37**, 8523.
237 M. G. Schwab, A. Narita, Y. Hernandez, T. Balandina, K. S. Mali, S. De Feyter, X. Feng and K. Müllen, *J. Am. Chem. Soc.*, 2012, **134**, 18169.
238 M. El Gemayel, A. Narita, L. F. Dössel, R. S. Sundaram, A. Kiersnowski, W. Pisula, M. R. Hansen, A. C. Ferrari, E. Orgiu, X. Feng, K. Müllen and P. Samori, *Nanoscale*, 2014, **6**, 6301.
239 A. N. Abbas, B. Liu, A. Narita, L. F. Dössel, B. Yang, W. Zhang, J. Tang, K. L. Wang, H. J. Räder, X. Feng, K. Müllen and C. Zhou, *J. Am. Chem. Soc.*, 2015, **137**, 4453.
240 M. Saleh, M. Baumgarten, A. Mavrinskiy, T. Schäfer and K. Müllen, *Macromolecules*, 2010, **43**, 137.
241 T. H. Vo, M. Shekhirev, D. A. Kunkel, M. D. Morton, E. Berglund, L. Kong, P. M. Wilson, P. A. Dowben, A. Enders and A. Sinitskii, *Nat. Commun.*, 2014, **5**, 3189.
242 M. Saleh, PhD thesis, University of Mainz, Germany, 2010.
243 T. H. Vo, M. Shekhirev, A. Lipatov, R. A. Korlacki and A. Sinitskii, *Faraday Discuss.*, 2014, **173**, 105.
244 T. H. Vo, M. Shekhirev, D. A. Kunkel, F. Orange, M. J. F. Guinel, A. Enders and A. Sinitskii, *Chem. Commun.*, 2014, **50**, 4172.
245 U. Kumar and T. X. Neenan, *Macromolecules*, 1995, **28**, 124.
246 C. H. Fujimoto, M. A. Hickner, C. J. Cornelius and D. A. Loy, *Macromolecules*, 2005, **38**, 5010.
247 C. E. P. Villegas, P. B. Mendonça and A. R. Rocha, *Sci. Rep.*, 2014, **4**, 6579.
248 S. A. Jensen, R. Ulbricht, A. Narita, X. Feng, K. Müllen, T. Hertel, D. Turchinovich and M. Bonn, *Nano Lett.*, 2013, **13**, 5925.
249 A. N. Abbas, G. Liu, A. Narita, M. Orosco, X. Feng, K. Müllen and C. Zhou, *J. Am. Chem. Soc.*, 2014, **136**, 7555.
250 R. Konnerth, C. Cervetti, A. Narita, X. Feng, K. Müllen, A. Hoyer, M. Burghard, K. Kern, M. Dressel and L. Bogani, *Nanoscale*, 2015, DOI: 10.1039/C4NR07378A.
251 U. Zschieschang, H. Klauk, I. B. Müller, A. J. Strudwick, T. Hintermann, M. G. Schwab, A. Narita, X. Feng, K. Müllen and R. T. Weitz, *Adv. Electron. Mater.*, 2015, **1**, 1400010.
252 A. Narita, I. A. Verzhbitskiy, W. Frederickx, K. S. Mali, S. A. Jensen, M. R. Hansen, M. Bonn, S. De Feyter, C. Casiraghi, X. Feng and K. Müllen, *ACS Nano*, 2014, **8**, 11622.
253 S. Osella, A. Narita, M. G. Schwab, Y. Hernandez, X. Feng, K. Müllen and D. Beljonne, *ACS Nano*, 2012, **6**, 5539.
254 L. Lafferentz, F. Ample, H. Yu, S. Hecht, C. Joachim and L. Grill, *Science*, 2009, **323**, 1193.
255 L. Grill, M. Dyer, L. Lafferentz, M. Persson, M. V. Peters and S. Hecht, *Nat. Nanotechnol.*, 2007, **2**, 687.
256 M. Bieri, M. Treier, J. Cai, K. Aït-Mansour, P. Ruffieux, O. Groning, P. Groning, M. Kastler, R. Rieger, X. Feng, K. Müllen and R. Fasel, *Chem. Commun.*, 2009, 6919.
257 L. Lafferentz, V. Eberhardt, C. Dri, C. Africh, G. Comelli, F. Esch, S. Hecht and L. Grill, *Nat. Chem.*, 2012, **4**, 215.
258 M. Treier, C. A. Pignedoli, T. Laino, R. Rieger, K. Müllen, D. Passerone and R. Fasel, *Nat. Chem.*, 2011, **3**, 61.
259 M. Saleh, PhD thesis, University of Mainz, Germany, 2010.
260 S. Linden, D. Zhong, A. Timmer, N. Aghdassi, J. H. Franke, H. Zhang, X. Feng, K. Müllen, H. Fuchs, L. Chi and H. Zacharias, *Phys. Rev. Lett.*, 2012, **108**, 216801.
261 P. Ruffieux, J. Cai, N. C. Plumb, L. Patthey, D. Prezzi, A. Ferretti, E. Molinari, X. Feng, K. Müllen, C. A. Pignedoli and R. Fasel, *ACS Nano*, 2012, **6**, 6930.
262 R. Denk, M. Hohage, P. Zeppenfeld, J. Cai, C. A. Pignedoli, H. Söde, R. Fasel, X. Feng, K. Müllen, S. Wang, D. Prezzi, A. Ferretti, A. Ruini, E. Molinari and P. Ruffieux, *Nat. Commun.*, 2014, **5**, 4253.
263 M. Koch, F. Ample, C. Joachim and L. Grill, *Nat. Nanotechnol.*, 2012, **7**, 713.

264 J. van der Lit, M. P. Boneschanscher, D. Vanmaekelbergh, M. Ijäs, A. Uppstu, M. Ervasti, A. Harju, P. Liljeroth and I. Swart, *Nat. Commun.*, 2013, **4**, 2023.
265 H. Huang, D. Wei, J. Sun, S. L. Wong, Y. P. Feng, A. H. C. Neto and A. T. S. Wee, *Sci. Rep.*, 2012, **2**, 983.
266 P. Han, K. Akagi, F. Federici Canova, H. Mutoh, S. Shiraki, K. Iwaya, P. S. Weiss, N. Asao and T. Hitosugi, *ACS Nano*, 2014, **8**, 9181.
267 Y.-C. Chen, D. G. de Oteyza, Z. Pedramrazi, C. Chen, F. R. Fischer and M. F. Crommie, *ACS Nano*, 2013, **7**, 6123.
268 H. Zhang, H. Lin, K. Sun, L. Chen, Y. Zagranyarski, N. Aghdassi, S. Duhm, Q. Li, D. Zhong, Y. Li, K. Müllen, H. Fuchs and L. Chi, *J. Am. Chem. Soc.*, 2015, **137**, 4022.
269 N. Abdurakhmanova, N. Amsharov, S. Stepanow, M. Jansen, K. Kern and K. Amsharov, *Carbon*, 2014, **77**, 1187.
270 A. Basagni, F. Sedona, C. A. Pignedoli, M. Cattelan, L. Nicolas, M. Casarin and M. Sambi, *J. Am. Chem. Soc.*, 2015, **137**, 1802.
271 O. Endo, M. Nakamura, K. Amemiya and H. Ozaki, *Surf. Sci.*, 2015, **635**, 44.
272 C. Bronner, S. Stremlau, M. Gille, F. Braußе, A. Haase, S. Hecht and P. Tegeder, *Angew. Chem., Int. Ed.*, 2013, **52**, 4422.
273 Y. Zhang, Y. Zhang, G. Li, J. Lu, X. Lin, S. Du, R. Berger, X. Feng, K. Müllen and H.-J. Gao, *Appl. Phys. Lett.*, 2014, **105**, 023101.
274 P. B. Bennett, Z. Pedramrazi, A. Madani, Y.-C. Chen, D. G. de Oteyza, C. Chen, F. R. Fischer, M. F. Crommie and J. Bokor, *Appl. Phys. Lett.*, 2013, **103**, 253114.
275 C.-A. Palma, K. Diller, R. Berger, A. Welle, J. Björk, J. L. Cabellos, D. J. Mowbray, A. C. Papageorgiou, N. P. Ivleva, S. Matich, E. Margapoti, R. Niessner, B. Menges, J. Reichert, X. Feng, H. J. Räder, F. Klappenberger, A. Rubio, K. Müllen and J. V. Barth, *J. Am. Chem. Soc.*, 2014, **136**, 4651.
276 H. Sakaguchi, Y. Kawagoe, Y. Hirano, T. Iruka, M. Yano and T. Nakae, *Adv. Mater.*, 2014, **26**, 4134.
277 A. V. Talyzin, I. V. Anoshkin, A. V. Krasheninnikov, R. M. Nieminen, A. G. Nasibulin, H. Jiang and E. I. Kauppinen, *Nano Lett.*, 2011, **11**, 4352.
278 A. Chuvilin, E. Bichoutskaia, M. C. Gimenez-Lopez, T. W. Chamberlain, G. A. Rance, N. Kuganathan, J. Biskupek, U. Kaiser and A. N. Khlobystov, *Nat. Mater.*, 2011, **10**, 687.
279 T. W. Chamberlain, J. Biskupek, G. A. Rance, A. Chuvilin, T. J. Alexander, E. Bichoutskaia, U. Kaiser and A. N. Khlobystov, *ACS Nano*, 2012, **6**, 3943.
280 H. E. Lim, Y. Miyata, M. Fujihara, S. Okada, Z. Liu, Arifin, K. Sato, H. Omachi, R. Kitaura, S. Irle, K. Suenaga and H. Shinohara, *ACS Nano*, 2015, **9**, 5034.
281 S. Bandow, M. Takizawa, K. Hirahara, M. Yudasaka and S. Iijima, *Chem. Phys. Lett.*, 2001, **337**, 48.